Phosphorylation of Janus kinase 1 (JAK1) by AMP-activated protein kinase (AMPK) links energy sensing to anti-inflammatory signaling

Rutherford, Claire; Speirs, Claire; Williams, Jamie J L; Ewart, Marie Ann; Mancini, Sarah J.; Hawley, Simon A.

Published in:
Science Signaling

DOI:
10.1126/scisignal.aaf8566

Publication date:
2016

Document Version
Peer reviewed version

Science Signaling
AAAS
Submitted Manuscript: Confidential DAY MONTH YEAR

Rapid AMP-activated protein kinase (AMPK) phosphorylation of Janus kinase 1 (JAK1) links energy sensing to anti-inflammatory signaling

Authors: Claire Rutherford[1], Claire Speirs[1], Jamie J.L. Williams[2], Marie-Ann Ewart[1$], Sarah J. Mancini[1], Simon A. Hawley[3], Christian Delles[1], Benoit Viollet[4,5,6], Ana P. Costa-Pereira[7], George S. Baillie[1], Ian P. Salt[1*] and Timothy M. Palmer[2*]

One Sentence Summary: Inhibition of JAK1 signaling by AMPK-mediated phosphorylation.

Affiliations:

[1]Institute of Cardiovascular and Medical Sciences, College of Medical, Veterinary and Life Sciences, University of Glasgow, Glasgow G12 8QQ, UK.

[2]School of Pharmacy, University of Bradford, Bradford BD7 1DP, UK.

[3]Division of Cell Signaling and Immunology, University of Dundee, Dundee DD1 5EH, UK.

[4]INSERM, U1016, Institut Cochin, Paris, France.

[5]CNRS, UMR8104, Paris, France.

[6]Université Paris Descartes, Sorbonne Paris Cité, France.

[7]Faculty of Medicine, Department of Surgery and Cancer, Imperial College London, Hammersmith Hospital Campus, London W12 0NN, UK.

[$]Current affiliation: AvantiCell Science Ltd., Auchincruive, Ayr KA6 5HW, UK.

*To whom correspondence should be addressed: Email T.Palmer1@bradford.ac.uk and Ian.Salt@glasgow.ac.uk

Abstract: AMP-activated protein kinase (AMPK) is a pivotal regulator of metabolism at the cellular and organismal level. A growing body of evidence also supports an important role for AMPK in suppressing inflammation but the molecular mechanisms responsible remain unclear. Here we demonstrate that AMPK rapidly inhibits activation of the JAK-STAT pathway and its downstream sequelae by an IL-6 *trans*-signaling complex. *In vitro* kinase assays show that AMPK can directly phosphorylate two residues (Ser515, Ser518) within the JAK1 SH2 domain. AMPK activation enhances JAK1interaction with 14-3-3 proteins *in vitro*, an effect which requires Ser515 and Ser518 and is abolished in cells lacking AMPK activity. Furthermore, mutation of Ser515 and Ser518 abolishes the ability of AMPK to inhibit JAK-STAT signaling stimulated by an IL-6 *trans*-signaling complex or following expression of a constitutively active Val658Phe-mutated JAK1. Importantly, clinically utilized AMPK activators metformin and salicylate enhance endogenous JAK1 phosphorylation and inhibit STAT3 phosphorylation in primary vascular endothelial cells. Therefore our findings reveal a previously unappreciated mechanism by which JAK1 function can be directly regulated in response to metabolic stress and

provide a mechanistic rationale for potential utilization of AMPK activators in a range of diseases associated with enhanced activation of the JAK-STAT pathway.

Introduction

The Janus kinase–signal transducer and activator of transcription (JAK–STAT) pathway is utilized by a range of cytokines that control survival, proliferation and differentiation responses in diverse cell types. JAKs comprise a family of four cytoplasmic tyrosine kinases (JAK1-JAK3, Tyk2) that function as essential signaling components immediately downstream of receptors for many hematopoietic cytokines, such as granulocyte-macrophage colony-stimulating factor, erythropoietin, leptin, interferons (IFNs) and interleukins such as IL-6 *(1)(2)*. The IL-6 receptor comprises two distinct subunits, an IL-6-binding protein (IL-6Rα) and a 130 kDa signal-transducing subunit (gp130) which is shared by all IL-6-family cytokines *(2)*. The gp130 subunit is ubiquitously expressed while IL-6Rα expression is restricted to hepatocytes, monocytes, neutrophils and some B and T cell subsets. However, IL-6 can also bind to a soluble form of the receptor (sIL-6Rα) generated either by limited proteolytic cleavage of membrane-bound IL-6Rα or alternate splicing of IL-6Rα primary transcripts. The resulting sIL-6Rα/IL-6 "*trans*-signaling" complexes can then associate with gp130 on cells that do not express the membrane-bound IL-6R, thereby widening the spectrum of IL-6-responsive cells *(3)*.

IL-6 binding to the receptor complex results in the activation of gp130-bound JAKs. The activated JAKs are then able to phosphorylate specific Tyr residues within the receptor's cytoplasmic domain, which serve as docking sites for SH2 domain-containing proteins. The major intracellular mediators are the signal transducer and activator of transcription (STAT) proteins. IL-6 is capable of activating STAT1 and STAT3, although STAT3 activation has been observed to a greater extent than STAT1. Activation of STATs require their recruitment to specific JAK-phosphorylated Tyr residues on gp130 *via* their SH2 domain followed by JAK-mediated phosphorylation of a Tyr residue in the transactivation domain (Tyr705 on STAT3, Tyr701 on STAT1). Tyr-phosphorylated STATs then form dimers which can translocate to the nucleus to activate target gene transcription. IL-6 can also activate the extracellular signal-regulated kinase 1,2 (ERK1,2) and phosphatidylinositol 3-kinase pathways following recruitment of the Tyr phosphatase SHP2 to JAK-phosphorylated gp130 *(2)(4)*.

AMP-activated protein kinase (AMPK) is the highly conserved downstream component of a Ser/Thr protein kinase cascade involved in the regulation of metabolism**.** It was initially characterised as a Ser/Thr protein kinase allosterically activated by increases in intracellular AMP levels resulting from the decline in intracellular ATP that occurs following nutrient deprivation or hypoxia *(5)(6)*. AMPK is a heterotrimeric complex comprised of a catalytic α subunit and regulatory β and γ subunits. In mammals, isoforms of each subunit (α1, α2, β1, β2, γ1, γ2, γ3) are encoded by seven genes. The β subunits are each N-terminally myristoylated, contain carbohydrate-binding domains and interact with both the α and γ subunits, whereas the γ subunits contain the AMP/ADP binding sites responsible for sensing cellular energy status [reviewed in *(5)*]. In addition to the allosteric activation of AMPK by adenine nucleotides, AMP or ADP binding to the regulatory γ subunit of AMPK promotes phosphorylation of the catalytic α subunit at Thr172, which is required for AMPK activity. Binding of AMP and ADP also inhibits dephosphorylation of AMPK, maintaining Thr172 phosphorylation by the upstream AMPK Thr172 kinase, liver kinase B1 (LKB1) *(5)(6)*. In the absence of changes in adenine

nucleotide ratios, AMPK can be activated by increases in intracellular Ca^{2+} concentrations in cells expressing Ca^{2+}/calmodulin-dependent protein kinase kinase β (CaMKKβ) *(5)(6)*.

The most studied aspect of AMPK function is its role in maintaining cellular energy stores and regulating whole body energy balance. An important aspect of this role is the direct phosphorylation of metabolic enzymes such as acetyl coA carboxylase (ACC) 1 and 2, which catalyze the carboxylation of acetyl coA to malonyl-CoA, a key substrate for fatty acid biosynthesis that also inhibits free fatty acid transport into mitochondria *(7)*. AMPK-mediated phosphorylation of ACC1 on Ser79 inhibits its activity thereby suppressing fatty acid synthesis and enhancing β-oxidation *(8)*. An increasing body of evidence has revealed that AMPK is also an important regulator of inflammatory responses. For example, AMPK-dependent inhibition of tumor necrosis factor α (TNFα)-, lipopolysaccharide (LPS)- and interleukin-1β (IL-1β)-stimulated leukocyte recruitment to vascular endothelial cells *in vitro* has been observed in multiple studies, and is associated with reduced induction of adhesion molecules (e.g. VCAM-1 and E-selectin) and chemokines (e.g. CCL2 and CCL3) *(9)(10)*. Studies using AMPKα$1^{-/-}$ and AMPKα$2^{-/-}$ mice suggest that both isoforms can contribute to inhibition of post-ischemic leukocyte adhesion to blood vessels *in vivo* by the AMPK activator 5'-aminoimidazole-4-carboxamide ribonucleoside (AICAR) *(11)*. Consistent with a role for AMPK in suppressing inflammation *in vivo*, aortae from AMPKα$1^{-/-}$ mice have been shown to display enhanced angiotensin II-stimulated VCAM-1 expression *(12)*. Activation of AMPK with AICAR is also associated with reduced infiltration of inflammatory cells in rodent models of acute and chronic colitis *(13)*, lung injury *(14)* and autoimmune encephalomyelitis *(15)*. Furthermore, increased infiltration and activation of macrophages have been observed in adipose tissue from wild type mice transplanted with bone marrow from AMPKβ$1^{-/-}$ mice *(16)*. Therefore, taken as a whole, it has become clear that AMPK can limit inflammatory cell infiltration and activation in multiple settings.

While AMPK's ability to maintain fatty acid oxidation in macrophages has been proposed as an important mechanism by which it limits inflammation in macrophages *(16)*, several mechanisms have also been identified though which AMPK can directly inhibit pro-inflammatory signaling pathways. However, while several potential mechanisms have been proposed to explain AMPK-mediated inhibition of the NF-κB pathway in response to stimuli such as TNFα, LPS and IL-1 *(9)(17)*, relatively few studies have examined how the JAK-STAT pathway is controlled by AMPK. This is a particularly important issue to address given the pathological roles of enhanced JAK-STAT signaling in multiple chronic inflammatory conditions such as atherosclerosis, colitis and rheumatoid arthritis, as well as several cancers and hematological disorders driven by mutational activation of JAK isoforms *(1)(18)(19)(20)*.

In this study, we demonstrate that AMPK can rapidly and profoundly inhibit activation of the JAK-STAT pathway in response to multiple stimuli. In addition, we show that this occurs *via* a previously unappreciated mechanism involving direct AMPK-mediated phosphorylation of JAK1 within its regulatory SH2 domain. Our data therefore reveal how metabolic stress can rapidly control signaling from JAK1, and provide a molecular basis for potential repurposing of AMPK activators for a range of diseases associated with enhanced activation of the JAK-STAT pathway.

Results

AMPK rapidly inhibits IL-6 signaling and function

AMPK plays a largely protective role in vascular endothelial cells (ECs) *via* both NO-dependent and –independent mechanisms *(21)(22)*. Incubation of human umbilical vein ECs (HUVECs) with sIL-6Rα/IL-6 *trans*-signaling complexes for 30 min significantly increased STAT3 phosphorylation on Tyr705, an effect that was significantly inhibited in HUVECs that had been pre-incubated with distinct stimuli that each activate AMPK as determined by assessing ACC1 phosphorylation on Ser79 *(8)*: these were AICAR, which is phosphorylated intracellularly to the AMP mimetic ZMP *(23)*, A769662, which binds and activates β1-containing AMPK complexes *via* an AMP/ADP-independent mechanism *(24)*, and a combination of clinically utilized AMPK activators metformin and salicylate, which synergistically activate AMPK *via* elevation of cellular AMP levels and directly binding β1-subunits respectively *(25)(26)(27)* (Figure 1A). Under these conditions, AMPK activation on its own had no detectable effect on STAT3 phosphorylation. Targeted short inhibitory RNA (siRNA)-mediated knockdown of AMPKα1 catalytic subunits reduced the inhibitory effects of both A769662 (Figure 1B) and AICAR (Figure S1), indicating that these effects were mediated *via* AMPK activation. In addition, adenovirus (AV)-mediated expression of a catalytically inactive dominant negative (DN) AMPKα1 subunit in which Asp157 located within subdomain VII of the catalytic domain is mutated to Ala *(28)* was sufficient to block A769662-mediated inhibition of STAT3 phosphorylation in HUVECs *versus* a GFP-expressing control AV (Figure S1). Together, these data demonstrated that activation of AMPK by multiple stimuli triggered a rapid and significant reduction in the ability of sIL-6Rα/IL-6 to stimulate STAT3 phosphorylation on Tyr705.

To assess the functional consequences of AMPK-mediated inhibition of IL-6 signaling, we initially examined the effect of A769662 on IL-6-mediated induction of STAT3 target genes suppressor of cytokine signaling 3 (SOCS3) and CCAAT/enhancer binding protein δ (C/EBPδ) *(29)(30)*. Similar to the effect on STAT3 phosphorylation, A769662 significantly inhibited sIL-6Rα/IL-6-stimulated accumulation of SOCS3 and C/EBPδ protein (Figure 1C) and mRNA (Figure S2). In addition, we took advantage of the well described ability of IL-6 to induce chemokine expression and thereby increase monocyte chemotaxis *(20)(31)(32)*. Conditioned media was collected from HUVECs subsequent to stimulation in the presence or absence of A769662 and/or sIL-6Rα/IL-6 prior to assessment of its capacity to stimulate monocyte migration using a trans-well migration assay. Since the HUVECs were extensively washed to remove A769662 and sIL-6Rα/IL-6 prior to collection of conditioned medium, these had no effect on migration directly. It was found that the migration of U937 monocytic cells towards conditioned media from sIL-6Rα/IL-6-stimulated HUVECs was significantly increased. Conditioned medium from HUVECs pre-incubated with A769662 for 30 min prior to cytokine stimulation elicited significantly less U937 cell migration compared to conditioned media from sIL-6Rα/IL-6-stimulated HUVECs (Figure 1D).

AMPK inhibits signaling from multiple cytokine receptor complexes

To identify the point in the IL-6 signaling pathway at which AMPK was acting, we examined signaling downstream of multiple cytokines other cytokine receptors. Importantly, we found that the inhibitory effect of AMPK on sIL-6Rα/IL-6 responses was not restricted to STAT3, as pre-incubation of HUVECs with A769662 also abrogated sIL-6Rα/IL-6-stimulated phosphorylation of STAT1 on Tyr701 (Figure 2A). While IL-6 signals downstream *via* interaction with either a membrane-bound or sIL-Rα and gp130 homodimers, leukemia inhibitory factor (LIF) and oncostatin M (OSM) signal *via* cytokine interaction with gp130/LIF receptor (LIFR) and OSM

receptor/gp130 heterodimers respectively *(2)* Similar to sIL-6Rα/IL-6, pre-treatment of HUVECs with A769662 significantly reduced OSM- and LIF-stimulated STAT3 and STAT1 phosphorylation (Figure 2A). In addition, the ability of each cytokine to stimulate STAT3 phosphorylation on Ser727, which is critical for full transcriptional activation and is mediated by cytokine receptor activation of either ERK1,2 or phosphatidylinositol 3-kinase/mammalian target of rapamycin (mTOR) pathways, was similarly reduced by A769662 (Figure 2A). In support of a post-receptor effect of AMPK, A769662 also suppressed STAT3 phosphorylation in response to IFNα, which activates STATs *via* a distinct IFNα/β receptor 1 (IFNAR1)/IFNAR2 complex that lacks gp130 *(33)* (Figure 2B). Taken together, these results would suggest that AMPK exerts its inhibitory effects on multiple cytokine-activated signaling pathways at one or more common loci downstream of both IFNAR1/IFNAR2 and gp130-containing cytokine receptor complexes.

JAK1 is phosphorylated by AMPK in vitro

The IFNAR1/IFNAR2 complex couples to STATs *via* JAK1 and Tyk2 *(33)(34)*. We performed JAK1, JAK2 and Tyk2 siRNA knockdown experiments in HUVECs which demonstrated that JAK1 accounts for most of the ability of sIL-6Rα/IL-6 complexes to activate STAT3 (Figure S3). Thus JAK1 was identified as a potential common AMPK-regulated post-receptor target. As AMPK is a Ser/Thr protein kinase, and the inhibitory effect of AMPK activator A769662 occurred rapidly, we investigated the possibility that AMPK could directly phosphorylate JAK1. Peptide arrays of overlapping 25-mer peptides sequentially shifted by five amino acids and spanning the full human JAK1 open reading frame (residues 1-1154) were utilized for *in vitro* kinase assays with AMPK purified from rat liver and [γ^{32}P]ATP *(35)(36)*. These experiments identified a sequence within the JAK1 SH2 domain (R^{506}YSLHGSDRSFPSLGDLMSHLKKQI) as a potential substrate whose phosphorylation on the array was greater than that of the so-called "SAMS" peptide typically used as an *in vitro* substrate for assay of AMPK activity and which is based on the primary Ser79 AMPK phosphorylation site on rat ACC1 *(35)* (Figure 3A). To define which of the five potential phospho-acceptor sites within the JAK1 peptide were phosphorylated *in vitro* by AMPK, kinase assays were then performed on additional arrays containing the wild type (WT) peptide sequence and mutant peptides in which each Ser residue was replaced with a non-phosphorylatable Ala residue either individually or in combination (Figure 3B). Simultaneous replacement of all five Ser residues with Ala abolished AMPK-mediated phosphorylation of the peptide. Individual replacement of each Ser residue with Ala either did not alter or enhanced AMPK phosphorylation of the resulting peptides. However, simultaneous replacement of Ser515 and Ser518 with Ala abrogated peptide phosphorylation to the same extent as mutating all five Ser residues. In addition, a peptide in which Ser508, Ser512 and Ser524 were all replaced with Ala was phosphorylated to the same extent as the WT JAK1 sequence (Figure 3B). Taken together, these observations identified Ser515 and Ser518 in human JAK1 as potential sites of phosphorylation by AMPK *in vitro*.

Peptide library screening, mutagenesis and molecular modelling studies *(37)(38)* have all been used to identify optimal AMPK substrate motifs. Bioinformatic analysis of JAK1 orthologues revealed that phosphorylation sites equivalent to Ser518 in human JAK1 are conserved in multiple species (Figure 3C). Importantly, residues at positions +3 and +4 downstream of the phospho-acceptor sites which are known to be critical for substrate recognition are also well conserved (Figure 3C). Interestingly, Ser518 is located at the start of a specific α-helix conserved amongst all JAK isoforms (Figure 3D) *(39–41)*. In contrast, Ser515 is unique to human JAK1 and would only form a weak consensus for AMPK substrate recognition if Ser518

became negatively charged *via* prior phosphorylation (Figure 3C). However other examples of AMPK substrates that only loosely follow the optimized consensus have also been documented (e.g. eNOS phosphorylation at Ser633 *(42)*). Thus we examined a potential role for both Ser515 and Ser518 in more detail.

AMPK-mediated phosphorylation of JAK1 in intact cells

A common mechanism for phosphorylation-mediated regulation of target protein function is phosphorylation-dependent binding to members of the 14-3-3 family of proteins *(43)*. To assess whether phosphorylation of Ser515 and Ser518 could facilitate JAK1 interaction with 14-3-3 proteins *in vitro*, overlay assays were performed with horseradish peroxidase (HRP)-conjugated 14-3-3ζ (HRP-14-3-3ζ)and peptide arrays comprising 25-mer peptides from the identified JAK1 region in which either or both of Ser515 and Ser518 were phosphorylated (Figure 4A). These demonstrated that phospho-Ser515 and phospho-Ser518 peptides strongly interacted with HRP-14-3-3ζ *in vitro*, while no binding was detectable with either non-phosphorylated peptide or peptide in which both Ser515 and Ser518 were phosphorylated (Figure 4A).

A phosphorylation-dependent interaction with 14-3-3 proteins has been reported for several AMPK substrates, including Atg9, Raptor and ULK1 *(44)(38)(45)*. We tested our ability to detect any such interaction using two approaches. Firstly, we compared the ability of bacterially expressed and affinity purified GST/14-3-3 fusion proteins to capture AMPK-phosphorylated JAK1 in pull down assays from soluble extracts prepared from intact cells. Initial experiments in JAK1-null U4C human fibrosarcoma cells stably expressing recombinant JAK1 *(46)(47)* demonstrated that distinct GST/14-3-3 isoforms (14-3-3ζ and 14-3-3τ) but not GST alone could specifically isolate JAK1 (Figure S4). To assess the importance of Ser515 and Ser518 in mediating this interaction, we used a different approach in which WT and Ser515,518Ala (SSAA)-mutated human JAK1 were transiently expressed in U4C cells prior to immunoprecipitation of JAK1 and overlay of blots with HRP-14-3-3ζ. Consistent with the peptide array overlays, these experiments demonstrated that while WT JAK1 could be specifically identified, the SSAA-mutated JAK1 could not despite equivalent levels of JAK1 in the immunoprecipitates (Figure S4). Finally, to assess the role of AMPK activation on JAK1 phosphorylation in intact cells, WT and Ser515,518Ala (SSAA)-mutated human JAK1 were transiently expressed in U4C cells prior to treatment with A769662 and preparation of cell extracts for pull down assays with GST/14-3-3ζ and immunoblotting with anti-JAK1 antibody (Figure 4B). These demonstrated that A769662 treatment increased 14-3-3ζ interaction with JAK1 but not Ser515,518Ala (SSAA)-mutated JAK1 despite equivalent activation of AMPK and expression of WT and mutated JAK1 proteins in transfected cells (Figure 4B).

To further examine the AMPK dependence of this effect, GST/14-3-3ζ pull downs were performed in WT murine embryonic fibroblasts (MEFs) and MEFs with no detectable AMPK activity due to homozygous deletion of AMPKα1 and α2 catalytic subunits *(48)*. AMPK activation with A769662 in WT MEFs transiently increased interaction of endogenous JAK1 with GST/14-3-3ζ but this effect was absent in cells devoid of AMPK activity as determined by the loss of ACC phosphorylation on Ser79 (Figure 4C). As murine JAK1 lacks Ser515 or an equivalent residue (Figure 3C), this suggests that phosphorylation of Ser517 alone on murine JAK1 is required for interaction with GST/14-3-3ζ. Finally, we examined the effects of combined metformin and salicylate treatment on AMPK-mediated JAK1 phosphorylation (as determined by interaction with GST/14-3-3ζ) in HUVECs, a treatment which we had already

shown significantly inhibited sIL-6Rα/IL-6-stimulated STAT3 phosphorylation (Figure 1A). Combined treatment of HUVECs with metformin and salicylate significantly increased ACC phosphorylation and triggered a transient increase in endogenous JAK1 captured by GST/14-3-3ζ which peaked at 1 hr post-stimulation (Figure 4D).

AMPK-mediated inhibition of JAK1-dependent signaling requires Ser515 and Ser518

To investigate any contribution of AMPK-mediated JAK1 phosphorylation on Ser515 and Ser518 towards regulating signaling, we utilized JAK1-null U4C human fibrosarcoma cells. Consistent with previous work *(46)* and our own siRNA experiments in HUVECs, loss of JAK1 was associated with no detectable sIL-Rα/IL-6-mediated phosphorylation of STAT3. However, transient expression of WT human JAK1 was able to restore sIL-Rα/IL-6-mediated STAT3 phosphorylation over GFP-expressing controls and this was inhibited by pre-treatment with A769662 similar to the phenomenon observed in HUVECs (Figure 5A). Expression of SSAA-mutated JAK1 in U4C cells was also able to restore sIL-Rα/IL-6-mediated STAT3 phosphorylation, but the ability of A769662 to inhibit this effect was lost despite maintaining its ability to activate AMPK as measured by ACC phosphorylation (Figure 5B).

We then examined the effects of AMPK activation on signaling downstream of a constitutively active Val658Phe-mutated version of JAK1 found in patients with acute lymphoblastic leukemia (ALL) *(49)*. Analogous to the Val617Phe mutation in JAK2 responsible for several myeloproliferative neoplasms, this mutation within the JAK1 JH2 pseudokinase domain is thought to relieve an auto-inhibitory interaction with the catalytic JH1 domain, thereby increasing Tyr kinase activity independent of cytokine stimulation *(1)(50)*. In contrast to WT JAK1, transient expression of Val658Phe JAK1 in JAK1-null U4C cells was sufficient to trigger detectable Tyr phosphorylation of both STAT1 and STAT3 in the absence of added cytokine (Figure 5C). Importantly, treatment with A769662 increased ACC phosphorylation and inhibited STAT1 and STAT3 Tyr phosphorylation. Expression of Val658Phe JAK1 incorporating the Ser515,518Ala (SSAA) mutations also resulted in increased basal STAT phosphorylation, although this was less than with Val658Phe JAK1. However, A769662 treatment failed to significantly inhibit the response despite increasing ACC phosphorylation (Figure 5C). Together, these observations suggest that Ser515 and Ser518 are required for effective AMPK-mediated inhibition of JAK1-mediated downstream signaling to STAT1 and STAT3.

Discussion

It is becoming increasingly apparent that cells can couple inflammatory status to the availability of nutrients *(51)(52)*. Conversely, the mechanisms by which nutrient availability can regulate inflammation remain unclear. In this study we demonstrate that direct phosphorylation of JAK1, a key signaling intermediate utilized by a variety of cytokines, can occur in response to stimulation of AMPK, a key determinant of cellular energy status, by multiple activators. In conjunction with other observations, this would suggest that energy stress triggers an LKB1-dependent activation of AMPK that can inhibit the JAK-STAT pathway *via* several distinct mechanisms. For example, others have shown that chronic AMPK activation in hepatocytes with metformin for 12 hr is able to increase levels of the orphan nuclear receptor small heterodimer partner (SHP), which reduces STAT3 phosphorylation on Tyr705 and co-localizes with nuclear STAT3 to reduce its binding to target gene promoters *(53)(54)*. Similarly, others have demonstrated that chronic treatment of hepatocytes with AICAR suppresses IL-6 signaling, and

was thought to involve an AMPK-mediated inhibition of IL-6-stimulated Tyr phosphorylation and activation of JAK1 and JAK2, and that depletion of AMPKα1 and α2 subunits could block the inhibitory effects of AMPK activators on cytokine-stimulated signaling without significantly altering basal activation *(55)(56)*. However the underlying mechanisms were not investigated. Finally, a role for AMPK-mediated induction of mitogen-activated protein kinase phosphatase-1 (MKP-1) has been reported to play a critical role in suppressing STAT1 activation in aortic smooth muscle cells *(57)*. In contrast, we have demonstrated that AMPK-mediated phosphorylation of JAK1 within its regulatory SH2 domain is a rapid event mediated by direct AMPK activators (A769662, salicylate) and mitochondrial inhibitors (metformin) and is required for AMPK to inhibit STAT3 activation by IL-6 in multiple cell systems. The location of the conserved Ser518 residue at the start of the αB helix within the JAK1 SH2 domain *(39)* suggests that phosphorylation may disrupt SH2 domain structure sufficiently to uncouple cytokine receptors from JAK1 activation, although this has yet to be tested. We also found that either AMPKα1 knockdown or AV-mediated expression of dominant negative AMPKα1 specifically blocked the ability of AMPK activators to suppress STAT, thereby ruling out a constitutive suppressive effect of AMPK on JAK-STAT signaling under our conditions. Finally, the existence of several inhibitory mechanisms by which AMPK can control JAK-STAT signaling mirrors the multi-faceted impact of AMPK on the mTOR signaling pathway, which it controls *via* direct phosphorylation of two components (TSC2 on Ser1387 *(58)(59)*, Raptor on Ser722 and Ser792 *(38)*). These observations suggest that, like the mTOR pathway, AMPK-mediated regulation of JAK-STAT signaling has also evolved such that multiple mechanisms and targets are used to limit its activation.

Given the importance of AMPK and JAK-STAT signaling pathways in controlling processes such as cell proliferation, longevity, angiogenesis and inflammation, AMPK-mediated JAK1 phosphorylation could potentially influence these events. Several studies have reported that LKB1, the major kinase responsible for activation loop phosphorylation of AMPKα subunits in response to energy stress, exerts a suppressive effect on STAT3 phosphorylation and function, such that loss of LKB1 increases STAT3 phosphorylation *(60)(61)(62)*. LKB1 is a tumor suppressor and is frequently inactivated in human cancers *(63)*, while hyperactivation of STAT3 within tumor cells and the tumor microenvironment has been extensively described *(18)*. The identification of JAK1 as a target would suggest that AMPK activation might be a useful strategy for limiting STAT3-mediated tumor progression, in addition to its well described effects on cell growth, proliferation and autophagy *(45)(38)(64)*. The ability of AMPK to inhibit STAT phosphorylation following expression of a constitutively active Val658Phe-mutant of JAK1 *via* a mechanism requiring Ser515/518 would also support clinical studies to evaluate AMPK activators such as metformin as potential treatment options for ALL caused by activating JAK1 mutations *(49)(65)*.

Materials and Methods

Materials

Antibodies against JAK1 were from BD Transduction Laboratories [cat. no. 610232]. HRP-conjugated anti-GST antibodies were from Abcam [cat. no. ab3416]. Cytokines and HRP-conjugated 14-3-3ζ were from R&D Systems. Other antibodies used have been described elsewhere *(66)(67)(68)(21)(69)*. Peptide arrays were synthesized on glass slides by automatic

SPOT synthesis using Fmoc (9-fluorenylmethyloxycarbonyl) chemistry with the AutoSpot-Robot ASS 222 [Intavis Bioanalytical Instruments]. AMPK preparations used for *in vitro* kinase assays were purified from rat liver as previously described *(35)*. Ad5 adenoviruses expressing either GFP (AV.GFP) or a dominant negative mutant AMPKα1 (AV.DN-AMPKα1) were prepared, titered and used to infect HUVECs as described previously*(28)(68)(70)*

Cell culture and transfections

SV40-immortalised WT and AMPKα1$^{-/-}$α2$^{-/-}$ MEFs, HUVECs, U937 promonocytic cells and the human fibrosarcoma cell lines 2C4, U4C and U4C.JAK1 were cultured as previously described *(34)(47)(48)(21)(71)*. Transient expression of WT and mutated JAK1 constructs in U4C cells was performed using PolyFect transfection reagent [Qiagen] in accordance with the manufacturer's instructions. Transfection of HUVECs with siRNAs was performed as we have previously described *(71)(72)*.

Expression constructs

pGEX4T/14-3-3ζ was obtained from Professor Graeme Milligan (University of Glasgow, UK). C-terminally Flag- and myc epitope-tagged human JAK1 in pCMV6 was obtained from Origene [cat. no. RC213878]. QuikChange mutagenesis [Agilent Technologies] was used to introduce JAK1 mutations at Ser515/518 to Ala, and Val658 to Phe. All constructs were sequenced in their entirety to ensure that no additional unanticipated mutations had been introduced.

SDS-PAGE, immunoblotting and overlays

Cells were washed twice with ice-cold PBS and lysed by scraping into lysis buffer (50 mM HEPES pH 7.4, 150 mM sodium chloride, 1% (v/v) Triton X-100, 0.5% (v/v) sodium deoxycholate, 0.1% (w/v) SDS, 10 mM sodium fluoride, 5mM EDTA, 10 mM sodium phosphate, 0.1 mM phenylmethylsulfonyl fluoride (PMSF), 10 μg/ml benzamidine, 10 μg/ml soybean trypsin inhibitor, 2% (w/v) EDTA-free complete protease inhibitor cocktail [Sigma]). After 30 min on ice, lysates were vortexed and cleared by centrifugation. Equivalent amounts of protein, as determined by bicinchoninic acid protein assay, were fractionated by 8 to 12% SDS-PAGE gels depending on the application, transferred to a nitrocellulose membrane and analyzed either by immunoblotting or overlay with HRP-14-3-3ζ as previously described *(68)(71)*. Peptide arrays were blocked in 5% (w/v) BSA in Tris-buffered saline containing 0.1% (v/v) Tween-20 (TBST) prior to overlay with HRP-14-3-3ζ (1:500 in BSA/TBST) overnight at 4^{o}C, washing and visualization by enhanced chemiluminescence.

Peptide array AMPK assays

Peptide arrays were synthesized as previously described *(73)* AMPK phosphorylation of immobilized peptide arrays spotted in duplicate was undertaken with either vehicle or 0.5 units/ml of purified rat liver AMPK *(35)* diluted in phosphorylation buffer (50 mM HEPES, pH7.4, 0.01% (v/v) Brij-35, 1 mM DTT, 1 mM ATP, 0.2 mM AMP, 25 mM $MgCl_2$, 1% (w/v) BSA) containing 1 μCi [γ^{32}P]ATP followed by incubation at 30°C for 30 min. Phosphorylated peptides were visualized by autoradiography.

Pull-down assays and immunoprecipitations

Recombinant GST, GST/14-3-3τ and GST/14-3-3ζ were produced following induction in *E. coli* BL21 cells and purified from clarified bacterial extracts using glutathione-Sepharose beads. 20 μg of GST, GST/14-3-3τ or GST/14-3-3ζ immobilized on glutathione-Sepharose beads were

added to protein-equalized clarified cell extracts prepared in pull down assay buffer (50 mM HEPES, pH 7.4, 120 mM NaCl, 5 mM EDTA, 10% (v/v) glycerol, 1% (v/v) Triton X-100, supplemented with phosphatase inhibitors 5mM sodium fluoride, 1mM sodium orthovanadate, and protease inhibitors 10 μg/ml benzamidine, 0.1mM PMSF, 10 μg/ml soybean trypsin inhibitor, 2% (w/v) EDTA-free complete protease inhibitor cocktail) and incubated overnight with rotation at 4^{o}C. After washing three times in pull down assay buffer, samples were eluted in SDS-PAGE sample buffer by incubation at 65^{o}C for 30 min prior to fractionation on 8% SDS-PAGE gels and immunoblotting with anti-JAK1 antibody. GST fusion proteins were identified either by probing with HRP-conjugated anti-GST or Ponceau staining of nitrocellulose blots.

Flag-tagged WT and mutated human JAK1 were immunoprecipitated from transfected U4C cells solubilized in immunoprecipitation buffer using Flag M2-Sepharose beads prior to analysis by SDS-PAGE and immunoblotting as previously described *(73)*.

Analysis of conditioned medium for chemotactic activity

Conditioned medium was obtained from HUVECs pre-incubated in the presence or absence of 100 μM A769662 for 30 min prior to incubation with 25 ng/ml sIL-6Rα and 5 ng/ml IL-6 for 2 h. HUVECs were washed prior to collection of conditioned medium for 1h (such that residual sIL-6Rα/IL-6 and A769662 were not in conditioned medium). Conditioned medium from each treatment was then added to the bottom wells of a Boyden chamber and equal numbers of U937 promonocytic cells added to the top chamber, which was separated from the bottom by a collagen-coated membrane. After 5 hr, migrated U937 cells were collected from the lower well and counted in urinalysis glasstic slides [Stratagene, Cambridge, UK].

Statistical Analysis

Results are expressed as mean ± SEM. Statistically significant differences were determined using a two-tail t-test, or one or two-way ANOVA where appropriate, with $p < 0.05$ as significant.

Supplementary Materials

Fig. S1. AMPK-dependence of inhibition of STAT3 phosphorylation in HUVECs.

Fig. S2. AMPK inhibition of sIL-6Rα/IL-6-stimulated *SOCS3* and *CEBPD* mRNA induction.

Fig. S3. Contributions of JAK1, JAK2 and Tyk2 in mediating sIL-6Rα/IL-6-mediated STAT3 phosphorylation in HUVECs.

Fig. S4. Specific interaction of JAK1 with 14-3-3ζ and τ.

References and Notes

1. J. J. O'Shea, D. M. Schwartz, A. V Villarino, M. Gadina, I. B. McInnes, A. Laurence, The JAK-STAT pathway: impact on human disease and therapeutic intervention., *Annu. Rev. Med.* **66**, 311–28 (2015).

2. C. Garbers, H. M. Hermanns, F. Schaper, G. Müller-Newen, J. Grötzinger, S. Rose-John, J. Scheller, Plasticity and cross-talk of interleukin 6-type cytokines., *Cytokine Growth Factor Rev.* **23**, 85–97 (2012).

3. S. A. Jones, J. Scheller, S. Rose-John, Therapeutic strategies for the clinical blockade of IL-6/gp130 signaling., *J. Clin. Invest.* **121**, 3375–83 (2011).

4. R. Eulenfeld, A. Dittrich, C. Khouri, P. J. Müller, B. Mütze, A. Wolf, F. Schaper, Interleukin-6 signalling: more than Jaks and STATs., *Eur. J. Cell Biol.* **91**, 486–95 (2012).

5. D. G. Hardie, AMP-activated protein kinase: maintaining energy homeostasis at the cellular and whole-body levels., *Annu. Rev. Nutr.* **34**, 31–55 (2014).

6. G. R. Steinberg, B. E. Kemp, AMPK in Health and Disease., *Physiol. Rev.* **89**, 1025–78 (2009).

7. L. Tong, Structure and function of biotin-dependent carboxylases, *Cell. Mol. Life Sci.* **70**, 863–891 (2013).

8. K. Marcinko, G. R. Steinberg, The role of AMPK in controlling metabolism and mitochondrial biogenesis during exercise, *Exp. Physiol.* **99**, 1581–1585 (2014).

9. E. Bess, B. Fisslthaler, T. Frömel, I. Fleming, Nitric oxide-induced activation of the AMP-activated protein kinase α2 subunit attenuates IκB kinase activity and inflammatory responses in endothelial cells., *PLoS One* **6**, e20848 (2011).

10. B. Gongol, T. Marin, I.-C. Peng, B. Woo, M. Martin, S. King, W. Sun, D. A. Johnson, S. Chien, J. Y.-J. Shyy, AMPKα2 exerts its anti-inflammatory effects through PARP-1 and Bcl-6., *Proc. Natl. Acad. Sci. U. S. A.* **110**, 3161–6 (2013).

11. F. S. Gaskin, K. Kamada, M. Y. Zuidema, A. W. Jones, L. J. Rubin, R. J. Korthuis, Isoform-selective 5'-AMP-activated protein kinase-dependent preconditioning mechanisms to prevent postischemic leukocyte-endothelial cell adhesive interactions., *Am. J. Physiol. Heart Circ. Physiol.* **300**, H1352–60 (2011).

12. S. Schuhmacher, M. Foretz, M. Knorr, T. Jansen, M. Hortmann, P. Wenzel, M. Oelze, A. L. Kleschyov, A. Daiber, J. F. Keaney, G. Wegener, K. Lackner, T. Münzel, B. Viollet, E. Schulz, α1AMP-activated protein kinase preserves endothelial function during chronic angiotensin II treatment by limiting Nox2 upregulation., *Arterioscler. Thromb. Vasc. Biol.* **31**, 560–6 (2011).

13. A. Bai, M. Yong, A. G. Ma, Y. Ma, C. R. Weiss, Q. Guan, C. N. Bernstein, Z. Peng, Novel anti-inflammatory action of 5-aminoimidazole-4-carboxamide ribonucleoside with protective effect in dextran sulfate sodium-induced acute and chronic colitis., *J. Pharmacol. Exp. Ther.* **333**, 717–25 (2010).

14. X. Zhao, J. W. Zmijewski, E. Lorne, G. Liu, Y.-J. Park, Y. Tsuruta, E. Abraham, Activation of AMPK attenuates neutrophil proinflammatory activity and decreases the severity of acute lung injury., *Am. J. Physiol. Lung Cell. Mol. Physiol.* **295**, L497–504 (2008).

15. R. Prasad, S. Giri, N. Nath, I. Singh, A. K. Singh, 5-aminoimidazole-4-carboxamide-1-beta-4-ribofuranoside attenuates experimental autoimmune encephalomyelitis via modulation of endothelial-monocyte interaction., *J. Neurosci. Res.* **84**, 614–25 (2006).

16. S. Galic, M. D. Fullerton, J. D. Schertzer, S. Sikkema, K. Marcinko, C. R. Walkley, D. Izon, J. Honeyman, Z.-P. Chen, B. J. van Denderen, B. E. Kemp, G. R. Steinberg, Hematopoietic AMPK β1 reduces mouse adipose tissue macrophage inflammation and insulin resistance in obesity., *J. Clin. Invest.* **121**, 4903–15 (2011).

17. Y. Zhang, J. Qiu, X. Wang, Y. Zhang, M. Xia, AMP-activated protein kinase suppresses endothelial cell inflammation through phosphorylation of transcriptional coactivator p300., *Arterioscler. Thromb. Vasc. Biol.* **31**, 2897–908 (2011).

18. H. Yu, H. Lee, A. Herrmann, R. Buettner, R. Jove, Revisiting STAT3 signalling in cancer: new and unexpected biological functions, *Nat. Rev. Cancer* **14**, 736–746 (2014).

19. W. Vainchenker, S. N. Constantinescu, JAK/STAT signaling in hematological malignancies., *Oncogene* **32**, 2601–13 (2013).

20. G. Ortiz-Muñoz, J. L. Martin-Ventura, P. Hernandez-Vargas, B. Mallavia, V. Lopez-Parra, O. Lopez-Franco, B. Muñoz-Garcia, P. Fernandez-Vizarra, L. Ortega, J. Egido, C. Gomez-Guerrero, Suppressors of cytokine signaling modulate JAK/STAT-mediated cell responses during atherosclerosis., *Arterioscler. Thromb. Vasc. Biol.* **29**, 525–31 (2009).

21. M.-A. Ewart, C. F. Kohlhaas, I. P. Salt, Inhibition of tumor necrosis factor alpha-stimulated monocyte adhesion to human aortic endothelial cells by AMP-activated protein kinase., *Arterioscler. Thromb. Vasc. Biol.* **28**, 2255–7 (2008).

22. B. Enkhjargal, S. Godo, A. Sawada, N. Suvd, H. Saito, K. Noda, K. Satoh, H. Shimokawa, Endothelial AMP-activated protein kinase regulates blood pressure and coronary flow responses through hyperpolarization mechanism in mice., *Arterioscler. Thromb. Vasc. Biol.* **34**, 1505–13 (2014).

23. J. M. Corton, J. G. Gillespie, S. A. Hawley, D. G. Hardie, 5-Aminoimidazole-4-Carboxamide Ribonucleoside. A Specific Method for Activating AMP-Activated Protein Kinase in Intact Cells?, *Eur. J. Biochem.* **229**, 558–565 (1995).

24. J. W. Scott, B. J. W. van Denderen, S. B. Jorgensen, J. E. Honeyman, G. R. Steinberg, J. S. Oakhill, T. J. Iseli, A. Koay, P. R. Gooley, D. Stapleton, B. E. Kemp, Thienopyridone drugs are selective activators of AMP-activated protein kinase beta1-containing complexes., *Chem. Biol.* **15**, 1220–30 (2008).

25. M. R. Owen, E. Doran, A. P. Halestrap, Evidence that metformin exerts its anti-diabetic effects through inhibition of complex 1 of the mitochondrial respiratory chain., *Biochem. J.* **348 Pt 3**, 607–14 (2000).

26. S. A. Hawley, M. D. Fullerton, F. A. Ross, J. D. Schertzer, C. Chevtzoff, K. J. Walker, M. W. Peggie, D. Zibrova, K. A. Green, K. J. Mustard, B. E. Kemp, K. Sakamoto, G. R. Steinberg, D. G. Hardie, The ancient drug salicylate directly activates AMP-activated protein kinase., *Science* **336**, 918–22 (2012).

27. R. J. Ford, M. D. Fullerton, S. L. Pinkosky, E. A. Day, J. W. Scott, J. S. Oakhill, A. L. Bujak, B. K. Smith, J. D. Crane, R. M. Blümer, K. Marcinko, B. E. Kemp, H. C. Gerstein, G. R. Steinberg, Metformin and salicylate synergistically activate liver AMPK, inhibit lipogenesis and improve insulin sensitivity., *Biochem. J.* **468**, 125–32 (2015).

28. A. Woods, D. Azzout-Marniche, M. Foretz, S. C. Stein, P. Lemarchand, P. Ferre, F. Foufelle, D. Carling, Characterization of the Role of AMP-Activated Protein Kinase in the Regulation of Glucose-Activated Gene Expression Using Constitutively Active and Dominant Negative Forms of the Kinase, *Mol. Cell. Biol.* **20**, 6704–6711 (2000).

29. J. Yang, J. Huang, M. Dasgupta, N. Sears, M. Miyagi, B. Wang, M. R. Chance, X. Chen, Y.

Du, Y. Wang, L. An, Q. Wang, T. Lu, X. Zhang, Z. Wang, G. R. Stark, Reversible methylation of promoter-bound STAT3 by histone-modifying enzymes., *Proc. Natl. Acad. Sci. U. S. A.* **107**, 21499–504 (2010).

30. C. A. Cantwell, E. Sterneck, P. F. Johnson, Interleukin-6-Specific Activation of the C/EBPδ Gene in Hepatocytes Is Mediated by Stat3 and Sp1, *Mol. Cell. Biol.* **18**, 2108–2117 (1998).

31. M. Jougasaki, T. Ichiki, Y. Takenoshita, M. Setoguchi, Statins suppress interleukin-6-induced monocyte chemo-attractant protein-1 by inhibiting Janus kinase/signal transducers and activators of transcription pathways in human vascular endothelial cells., *Br. J. Pharmacol.* **159**, 1294–303 (2010).

32. M. Romano, M. Sironi, C. Toniatti, N. Polentarutti, P. Fruscella, P. Ghezzi, R. Faggioni, W. Luini, V. van Hinsbergh, S. Sozzani, F. Bussolino, V. Poli, G. Ciliberto, A. Mantovani, Role of IL-6 and Its Soluble Receptor in Induction of Chemokines and Leukocyte Recruitment, *Immunity* **6**, 315–325 (1997).

33. E. C. Borden, G. C. Sen, G. Uze, R. H. Silverman, R. M. Ransohoff, G. R. Foster, G. R. Stark, Interferons at age 50: past, current and future impact on biomedicine., *Nat. Rev. Drug Discov.* **6**, 975–90 (2007).

34. M. C. Gauzzi, L. Velazquez, R. McKendry, K. E. Mogensen, M. Fellous, S. Pellegrini, Interferon- -dependent Activation of Tyk2 Requires Phosphorylation of Positive Regulatory Tyrosines by Another Kinase, *J. Biol. Chem.* **271**, 20494–20500 (1996).

35. S. A. Hawley, M. Davison, A. Woods, S. P. Davies, R. K. Beri, D. Carling, D. G. Hardie, Characterization of the AMP-activated Protein Kinase Kinase from Rat Liver and Identification of Threonine 172 as the Major Site at Which It Phosphorylates AMP-activated Protein Kinase, *J. Biol. Chem.* **271**, 27879–27887 (1996).

36. K. M. Brown, L. C. Y. Lee, J. E. Findlay, J. P. Day, G. S. Baillie, Cyclic AMP-specific phosphodiesterase, PDE8A1, is activated by protein kinase A-mediated phosphorylation., *FEBS Lett.* **586**, 1631–7 (2012).

37. J. W. Scott, D. G. Norman, S. A. Hawley, L. Kontogiannis, D. G. Hardie, Protein kinase substrate recognition studied using the recombinant catalytic domain of AMP-activated protein kinase and a model substrate., *J. Mol. Biol.* **317**, 309–23 (2002).

38. D. M. Gwinn, D. B. Shackelford, D. F. Egan, M. M. Mihaylova, A. Mery, D. S. Vasquez, B. E. Turk, R. J. Shaw, AMPK phosphorylation of raptor mediates a metabolic checkpoint., *Mol. Cell* **30**, 214–26 (2008).

39. R. Ferrao, H. J. A. Wallweber, H. Ho, C. Tam, Y. Franke, J. Quinn, P. J. Lupardus, The Structural Basis for Class II Cytokine Receptor Recognition by JAK1., *Structure* **24**, 897–905 (2016).

40. R. McNally, A. V. Toms, M. J. Eck, T. J. Boggon, Ed. Crystal Structure of the FERM-SH2 Module of Human Jak2, *PLoS One* **11**, e0156218 (2016).

41. H. J. A. Wallweber, C. Tam, Y. Franke, M. A. Starovasnik, P. J. Lupardus, Structural basis of recognition of interferon-α receptor by tyrosine kinase 2., *Nat. Struct. Mol. Biol.* **21**, 443–8 (2014).

42. Z. Chen, I.-C. Peng, W. Sun, M.-I. Su, P.-H. Hsu, Y. Fu, Y. Zhu, K. DeFea, S. Pan, M.-D.

Tsai, J. Y.-J. Shyy, AMP-activated protein kinase functionally phosphorylates endothelial nitric oxide synthase Ser633., *Circ. Res.* **104**, 496–505 (2009).

43. D. Bridges, G. B. G. Moorhead, 14-3-3 proteins: a number of functions for a numbered protein., *Sci. STKE* **2005**, re10 (2005).

44. V. K. Weerasekara, D. J. Panek, D. G. Broadbent, J. B. Mortenson, A. D. Mathis, G. N. Logan, J. T. Prince, D. M. Thomson, J. W. Thompson, J. L. Andersen, Metabolic-stress-induced rearrangement of the 14-3-3ζ interactome promotes autophagy via a ULK1- and AMPK-regulated 14-3-3ζ interaction with phosphorylated Atg9., *Mol. Cell. Biol.* **34**, 4379–88 (2014).

45. H. I. D. Mack, B. Zheng, J. M. Asara, S. M. Thomas, AMPK-dependent phosphorylation of ULK1 regulates ATG9 localization., *Autophagy* **8**, 1197–214 (2012).

46. M. Müller, J. Briscoe, C. Laxton, D. Guschin, A. Ziemiecki, O. Silvennoinen, A. G. Harpur, G. Barbieri, B. A. Witthuhn, C. Schindler, The protein tyrosine kinase JAK1 complements defects in interferon-alpha/beta and -gamma signal transduction., *Nature* **366**, 129–35 (1993).

47. D. Guschin, N. Rogers, J. Briscoe, B. Witthuhn, D. Watling, F. Horn, S. Pellegrini, K. Yasukawa, P. Heinrich, G. R. Stark, A major role for the protein tyrosine kinase JAK1 in the JAK/STAT signal transduction pathway in response to interleukin-6., *EMBO J.* **14**, 1421–9 (1995).

48. K. R. Laderoute, K. Amin, J. M. Calaoagan, M. Knapp, T. Le, J. Orduna, M. Foretz, B. Viollet, 5'-AMP-activated protein kinase (AMPK) is induced by low-oxygen and glucose deprivation conditions found in solid-tumor microenvironments., *Mol. Cell. Biol.* **26**, 5336–47 (2006).

49. C. G. Mullighan, J. Zhang, R. C. Harvey, J. R. Collins-Underwood, B. A. Schulman, L. A. Phillips, S. K. Tasian, M. L. Loh, X. Su, W. Liu, M. Devidas, S. R. Atlas, I.-M. Chen, R. J. Clifford, D. S. Gerhard, W. L. Carroll, G. H. Reaman, M. Smith, J. R. Downing, S. P. Hunger, C. L. Willman, JAK mutations in high-risk childhood acute lymphoblastic leukemia., *Proc. Natl. Acad. Sci. U. S. A.* **106**, 9414–8 (2009).

50. O. Silvennoinen, S. R. Hubbard, Molecular insights into regulation of JAK2 in myeloproliferative neoplasms., *Blood* **125**, 3388–92 (2015).

51. L. A. J. O'Neill, D. G. Hardie, Metabolism of inflammation limited by AMPK and pseudo-starvation., *Nature* **493**, 346–55 (2013).

52. M. Dandapani, D. G. Hardie, AMPK: opposing the metabolic changes in both tumour cells and inflammatory cells?, *Biochem. Soc. Trans.* **41**, 687–93 (2013).

53. Y. D. Kim, Y. H. Kim, Y. M. Cho, D. K. Kim, S. W. Ahn, J. M. Lee, D. Chanda, M. Shong, C. H. Lee, H. S. Choi, Metformin ameliorates IL-6-induced hepatic insulin resistance via induction of orphan nuclear receptor small heterodimer partner (SHP) in mouse models., *Diabetologia* **55**, 1482–94 (2012).

54. Y. D. Kim, Y.-H. Kim, S. Tadi, J. H. Yu, Y.-H. Yim, N. H. Jeoung, M. Shong, L. Hennighausen, R. A. Harris, I.-K. Lee, C.-H. Lee, H.-S. Choi, Metformin inhibits growth hormone-mediated hepatic PDK4 gene expression through induction of orphan nuclear receptor small heterodimer partner., *Diabetes* **61**, 2484–94 (2012).

55. A. Nerstedt, E. Cansby, M. Amrutkar, U. Smith, M. Mahlapuu, Pharmacological activation

of AMPK suppresses inflammatory response evoked by IL-6 signalling in mouse liver and in human hepatocytes., *Mol. Cell. Endocrinol.* **375**, 68–78 (2013).

56. A. Nerstedt, A. Johansson, C. X. Andersson, E. Cansby, U. Smith, M. Mahlapuu, AMP-activated protein kinase inhibits IL-6-stimulated inflammatory response in human liver cells by suppressing phosphorylation of signal transducer and activator of transcription 3 (STAT3), *Diabetologia* **53**, 2406–2416 (2010).

57. C. He, H. Li, B. Viollet, M.-H. Zou, Z. Xie, AMP-activated Protein Kinase Suppresses Vascular Inflammation in vivo by Inhibiting Signal Transducer and Activator of Transcription-1., *Diabetes* (2015), doi:10.2337/db15-0107.

58. K. Inoki, T. Zhu, K.-L. Guan, TSC2 Mediates Cellular Energy Response to Control Cell Growth and Survival, *Cell* **115**, 577–590 (2003).

59. R. J. Shaw, N. Bardeesy, B. D. Manning, L. Lopez, M. Kosmatka, R. A. DePinho, L. C. Cantley, The LKB1 tumor suppressor negatively regulates mTOR signaling., *Cancer Cell* **6**, 91–9 (2004).

60. A. Mukhopadhyay, K. C. Berrett, U. Kc, P. M. Clair, S. M. Pop, S. R. Carr, B. L. Witt, T. G. Oliver, Sox2 cooperates with Lkb1 loss in a mouse model of squamous cell lung cancer., *Cell Rep.* **8**, 40–9 (2014).

61. Y. Wang, W. Dai, X. Chu, B. Yang, M. Zhao, Y. Sun, Downregulation of LKB1 suppresses Stat3 activity to promote the proliferation of esophageal carcinoma cells, *Mol. Med. Rep.* **9**, 2400–2404 (2014).

62. D. W. Kim, H. K. Chung, K. C. Park, J. H. Hwang, Y. S. Jo, J. Chung, D. V Kalvakolanu, N. Resta, M. Shong, Tumor suppressor LKB1 inhibits activation of signal transducer and activator of transcription 3 (STAT3) by thyroid oncogenic tyrosine kinase rearranged in transformation (RET)/papillary thyroid carcinoma (PTC)., *Mol. Endocrinol.* **21**, 3039–49 (2007).

63. M. Momcilovic, D. B. Shackelford, Targeting LKB1 in cancer - exposing and exploiting vulnerabilities., *Br. J. Cancer* **113**, 574–84 (2015).

64. D. F. Egan, D. B. Shackelford, M. M. Mihaylova, S. Gelino, R. A. Kohnz, W. Mair, D. S. Vasquez, A. Joshi, D. M. Gwinn, R. Taylor, J. M. Asara, J. Fitzpatrick, A. Dillin, B. Viollet, M. Kundu, M. Hansen, R. J. Shaw, Phosphorylation of ULK1 (hATG1) by AMP-activated protein kinase connects energy sensing to mitophagy., *Science* **331**, 456–61 (2011).

65. E. Flex, V. Petrangeli, L. Stella, S. Chiaretti, T. Hornakova, L. Knoops, C. Ariola, V. Fodale, E. Clappier, F. Paoloni, S. Martinelli, A. Fragale, M. Sanchez, S. Tavolaro, M. Messina, G. Cazzaniga, A. Camera, G. Pizzolo, A. Tornesello, M. Vignetti, A. Battistini, H. Cavé, B. D. Gelb, J.-C. Renauld, A. Biondi, S. N. Constantinescu, R. Foà, M. Tartaglia, Somatically acquired JAK1 mutations in adult acute lymphoblastic leukemia., *J. Exp. Med.* **205**, 751–8 (2008).

66. W. A. Sands, H. D. Woolson, S. J. Yarwood, T. M. Palmer, Exchange protein directly activated by cyclic AMP-1-regulated recruitment of CCAAT/enhancer-binding proteins to the suppressor of cytokine signaling-3 promoter., *Methods Mol. Biol.* **809**, 201–14 (2012).

67. S. J. Yarwood, G. Borland, W. A. Sands, T. M. Palmer, Identification of CCAAT/enhancer-binding proteins as exchange protein activated by cAMP-activated transcription factors that mediate the induction of the SOCS-3 gene., *J. Biol. Chem.* **283**, 6843–53 (2008).

68. M. M. A. Safhi, C. Rutherford, C. Ledent, W. A. Sands, T. M. Palmer, Priming of signal transducer and activator of transcription proteins for cytokine-triggered polyubiquitylation and degradation by the A 2A adenosine receptor., *Mol. Pharmacol.* **77**, 968–78 (2010).

69. J. A. Reihill, M.-A. Ewart, I. P. Salt, The role of AMP-activated protein kinase in the functional effects of vascular endothelial growth factor-A and -B in human aortic endothelial cells., *Vasc. Cell* **3**, 9 (2011).

70. W. A. Sands, A. F. Martin, E. W. Strong, T. M. Palmer, Specific Inhibition of Nuclear Factor- B-Dependent Inflammatory Responses by Cell Type-Specific Mechanisms upon A2A Adenosine Receptor Gene Transfer, *Mol. Pharmacol.* **66**, 1147–1159 (2004).

71. H. D. Woolson, V. S. Thomson, C. Rutherford, S. J. Yarwood, T. M. Palmer, Selective inhibition of cytokine-activated extracellular signal-regulated kinase by cyclic AMP via Epac1-dependent induction of suppressor of cytokine signalling-3., *Cell. Signal.* **21**, 1706–15 (2009).

72. C. Rutherford, S. Childs, J. Ohotski, L. McGlynn, M. Riddick, S. MacFarlane, D. Tasker, S. Pyne, N. J. Pyne, J. Edwards, T. M. Palmer, Regulation of cell survival by sphingosine-1-phosphate receptor S1P1 via reciprocal ERK-dependent suppression of Bim and PI-3-kinase/protein kinase C-mediated upregulation of Mcl-1., *Cell Death Dis.* **4**, e927 (2013).

73. Y. Y. Sin, T. P. Martin, L. Wills, S. Currie, G. S. Baillie, Small heat shock protein 20 (Hsp20) facilitates nuclear import of protein kinase D 1 (PKD1) during cardiac hypertrophy., *Cell Commun. Signal.* **13**, 16 (2015).

74. B. Wang, H. Yang, Y.-C. Liu, T. Jelinek, L. Zhang, E. Ruoslahti, H. Fu, Isolation of High-Affinity Peptide Antagonists of 14-3-3 Proteins by Phage Display †, *Biochemistry* **38**, 12499–12504 (1999).

Acknowledgments: The authors thank Ritchie Williamson for generating the structure in Figure 3D, and Marcus Rattray and Anne Graham for critically reviewing the manuscript.

Funding: T.M.P., I.P.S., G.S.B. and C.D. were supported by project grants from the British Heart Foundation (PG 12/1/29276, PG/13/82/30483), Chief Scientist Office (ETM/226) and an equipment grant from Diabetes UK (BDA11/0004309). T.M.P. and C.D. were also supported by project grants from NHS Greater Glasgow and Clyde Research Endowment Fund (2011REFCH08) and Chest, Heart and Stroke Scotland (R10/A131). A.P.C.-P. was supported by the Experimental Cancer Medicine and Cancer Research UK Centres at Imperial College, London, U.K. C.S. and S.J.M. were supported by PhD studentships from Diabetes UK (BDA11/0004403 [C.S.], BDA09/0003948 [S.J.M.]).

Author contributions: C.R. and C.S. designed, performed and analyzed the majority of experiments. J.J.L.W. designed performed and analyzed the OSM and LIF experiments. M.-A.E. designed, performed and analyzed the chemotaxis experiments. S.J.M. and C.D. advised on the study concept and design. G.S.B., B.V., S.A.H. and A.C.-P. advised on aspects of study design that employed the experimental tools they provided. All listed authors critically revised the manuscript and approved the final version. T.M.P. and I.P.S. were responsible for study conception and design. T.M.P. drafted the article, is the guarantor of this work and, as such, had full access to all the data in the study and takes responsibility for the integrity of the data and the accuracy of the analysis.

Competing interests: None.

Data and materials availability: Not applicable.

Figures and Tables

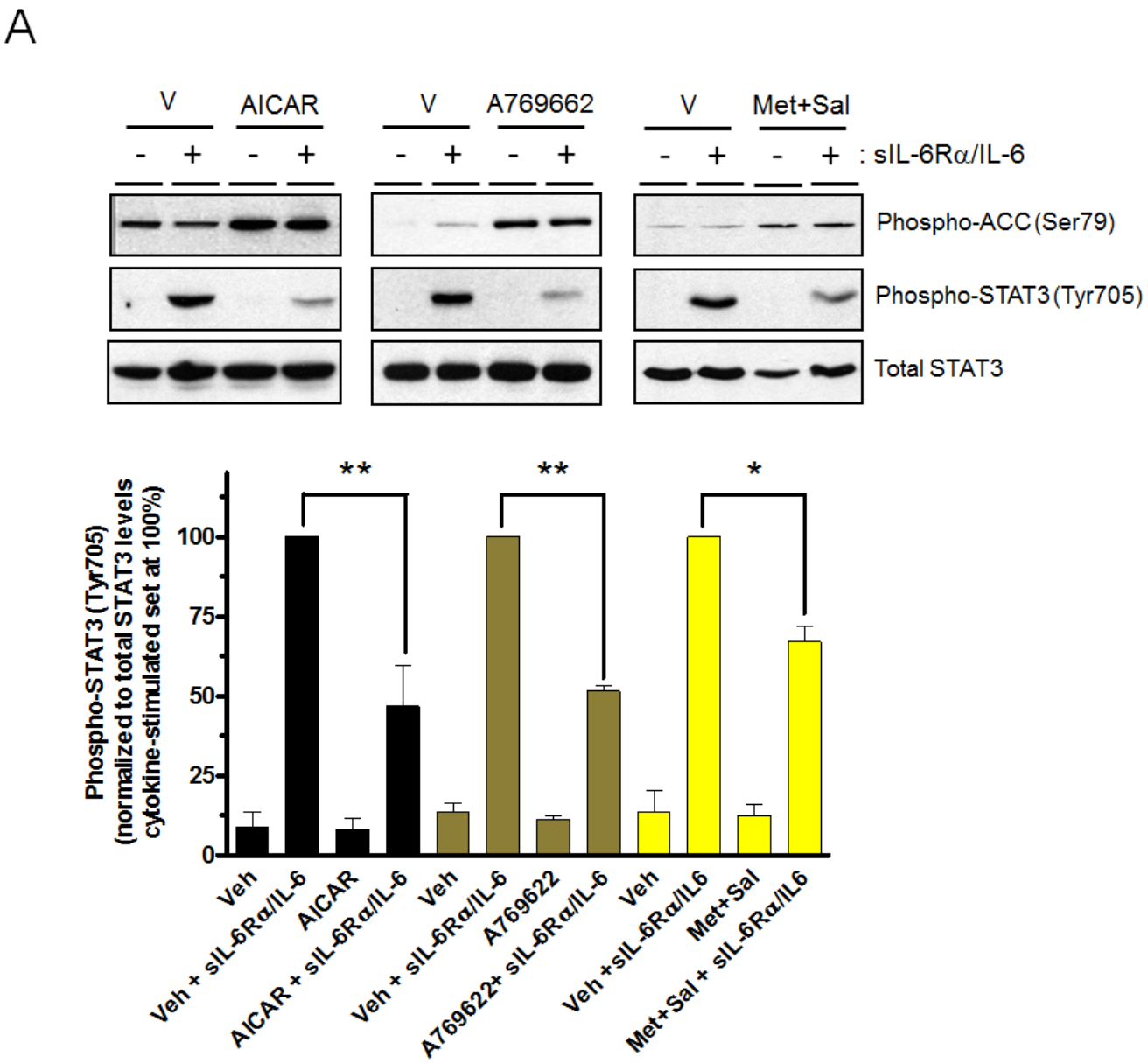

B

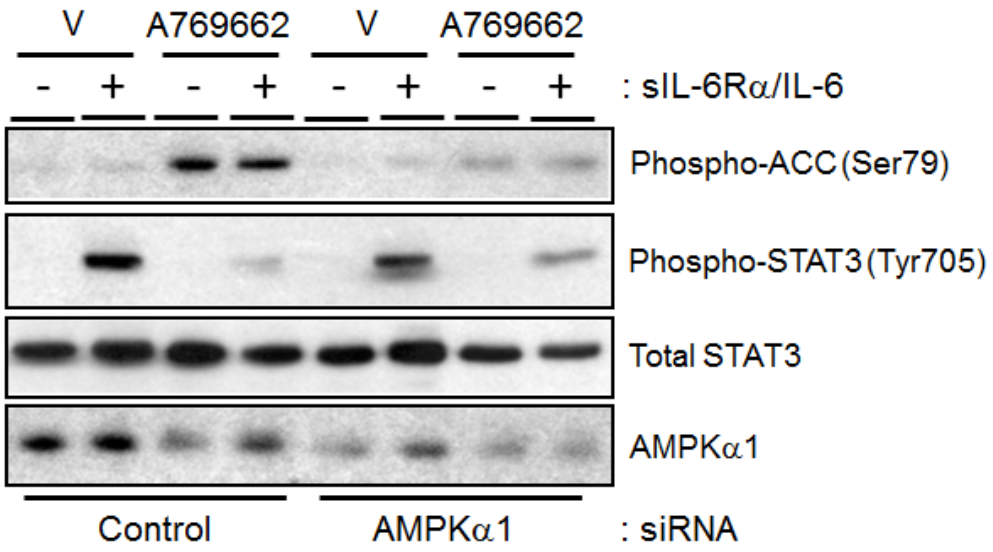
V
A769662
V
A769662
- + - + - + - +
: sIL-6Rα/IL-6
Phospho-ACC (Ser79)
Phospho-STAT3 (Tyr705)
Total STAT3
AMPKα1
Control
AMPKα1
: siRNA

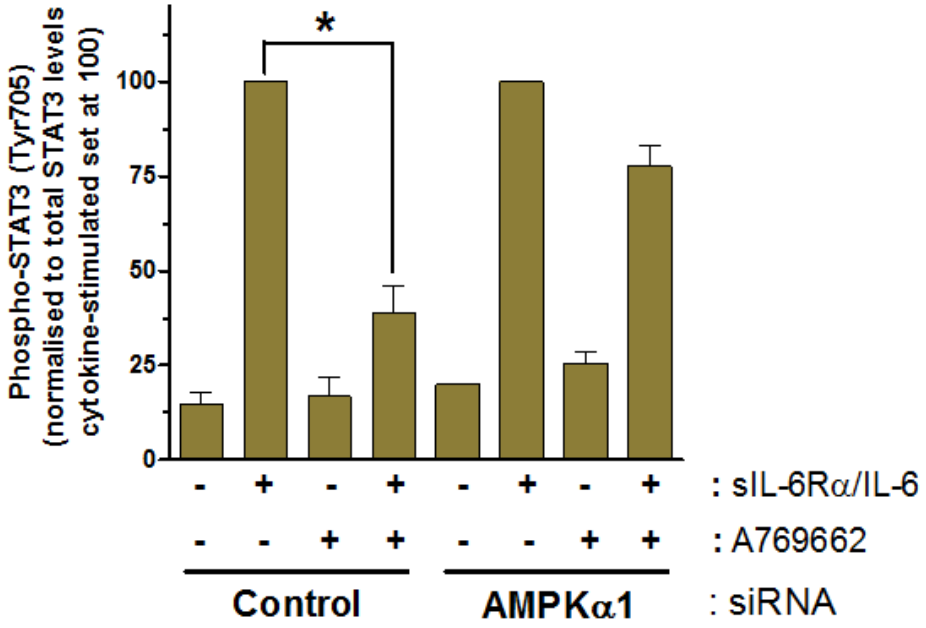
Phospho-STAT3 (Tyr705)
(normalised to total STAT3 levels
cytokine-stimulated set at 100)
*
100
75
50
25
0
- + - + - + - +
: sIL-6Rα/IL-6
- - + + - - + +
: A769662
Control
AMPKα1
: siRNA

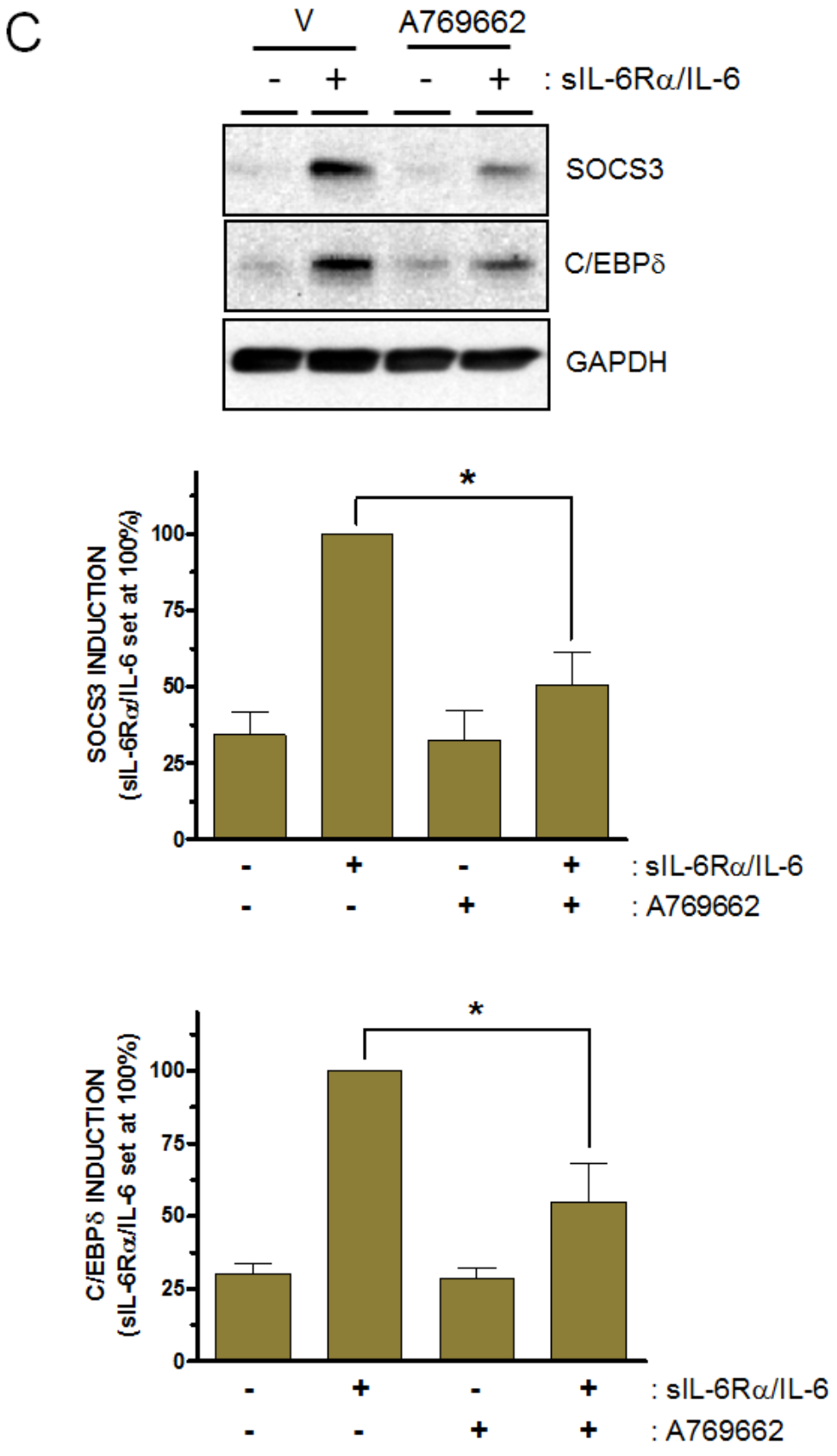
C
V
A769662
- + - + : sIL-6Rα/IL-6
SOCS3
C/EBPδ
GAPDH
SOCS3 INDUCTION
(sIL-6Rα/IL-6 set at 100%)
100
75
50
25
0
*
- + - + : sIL-6Rα/IL-6
- - + + : A769662
C/EBPδ INDUCTION
(sIL-6Rα/IL-6 set at 100%)
100
75
50
25
0
*
- + - + : sIL-6Rα/IL-6
- - + + : A769662

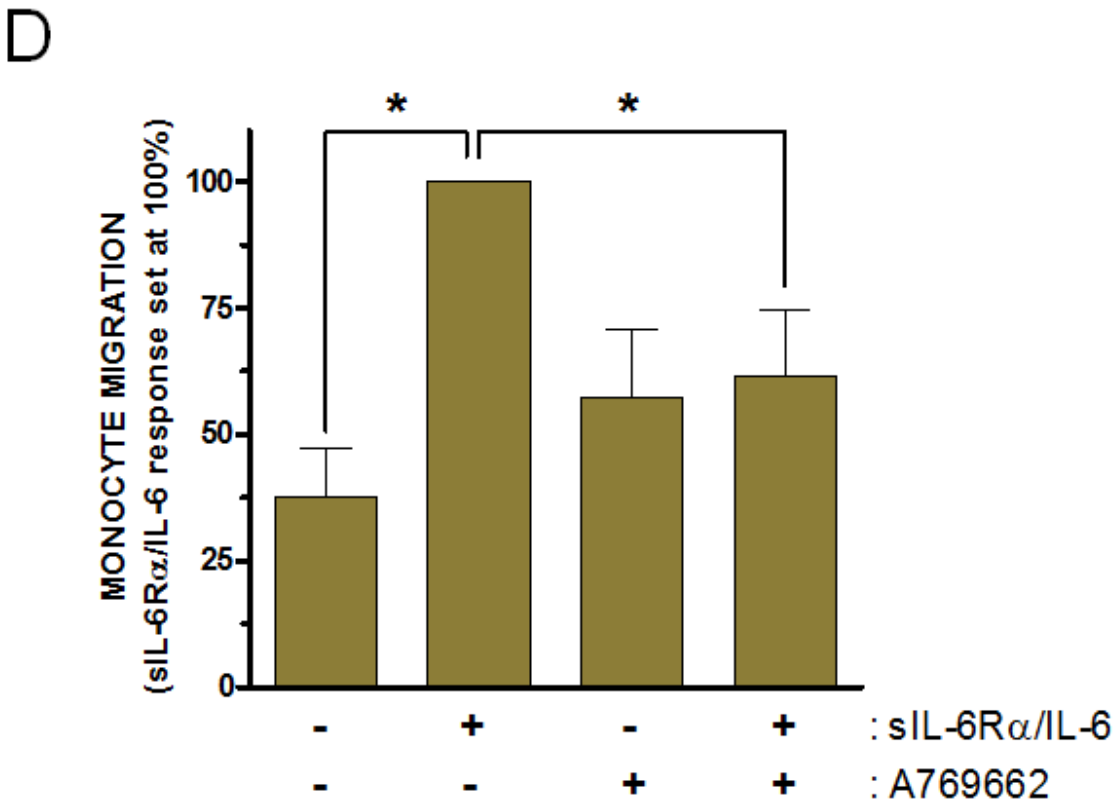

Fig. 1. **AMPK rapidly inhibits IL-6 signaling and function.** (**A**) HUVECs were pre-incubated in the presence or absence of 1 mM AICAR (2 hr), 100 μM A769662 (40 min) or a combination of 3 mM metformin and 5 mM salicylate (Met+Sal, 1 hr) prior to stimulation with sIL-6Rα/IL-6 (25 ng/ml, 5 ng/ml) for a further 30 min as indicated. Protein-equalized cell lysates were then analyzed by SDS-PAGE and immunoblotting with the indicated antibodies. Densitometric analysis for STAT3 phosphorylation normalized to respective total levels is shown in each case. Data are shown as mean ±SEM for N=3 independent experiments. **p<0.01, *p<0.05. (**B**) HUVECs were transfected with either non-targeting control or AMPKα1-specific siRNAs as indicated. Cells were then pre-incubated in the presence or absence of 100 μM A769662 (40 min) prior to stimulation with sIL-6Rα/IL-6 (25 ng/ml, 5 ng/ml) for a further 30 min as indicated. Protein-equalized cell lysates were then analyzed by SDS-PAGE and immunoblotting with the indicated antibodies. Densitometric analysis for STAT3 phosphorylation normalized to respective total levels is shown in each case. Data are shown as mean ±SEM for N=3 independent experiments. *p<0.05. (**C**) HUVECs were pre-treated for 40 min with or without A769662 (100 μM) prior to stimulation with sIL-6Rα/IL-6 (25 ng/ml, 5 ng/ml) for 5 hr. Cell lysates were then analyzed by SDS-PAGE and immunoblotting with the indicated antibodies. Densitometric analysis of N=3 independent experiments for SOCS3 and C/EBPδ normalized to GAPDH levels is shown. *p<0.05. (**C**) HUVECs were pre-treated for 30 min with or without A769662 (100 μM) prior to stimulation with sIL-6Rα/IL-6 (25 ng/ml, 5 ng/ml) for 2 hr. After washing and

incubation in fresh medium for a further 1 hr, conditioned medium was removed and used for chemotaxis assays using U937 promonocytic cells. Data are shown as mean ±SEM for N=3 independent experiments. *$p<0.05$.

A

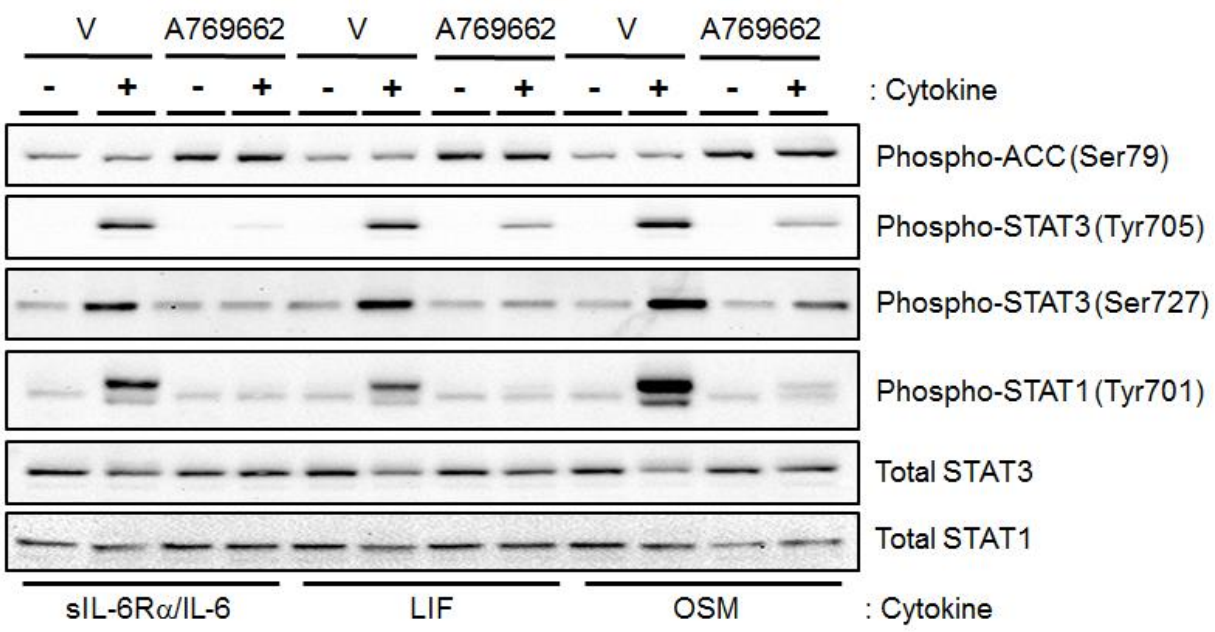
V
A769662
V
A769662
V
A769662
- + - + - + - + - + - +
: Cytokine
Phospho-ACC (Ser79)
Phospho-STAT3 (Tyr705)
Phospho-STAT3 (Ser727)
Phospho-STAT1 (Tyr701)
Total STAT3
Total STAT1
sIL-6Rα/IL-6
LIF
OSM
: Cytokine

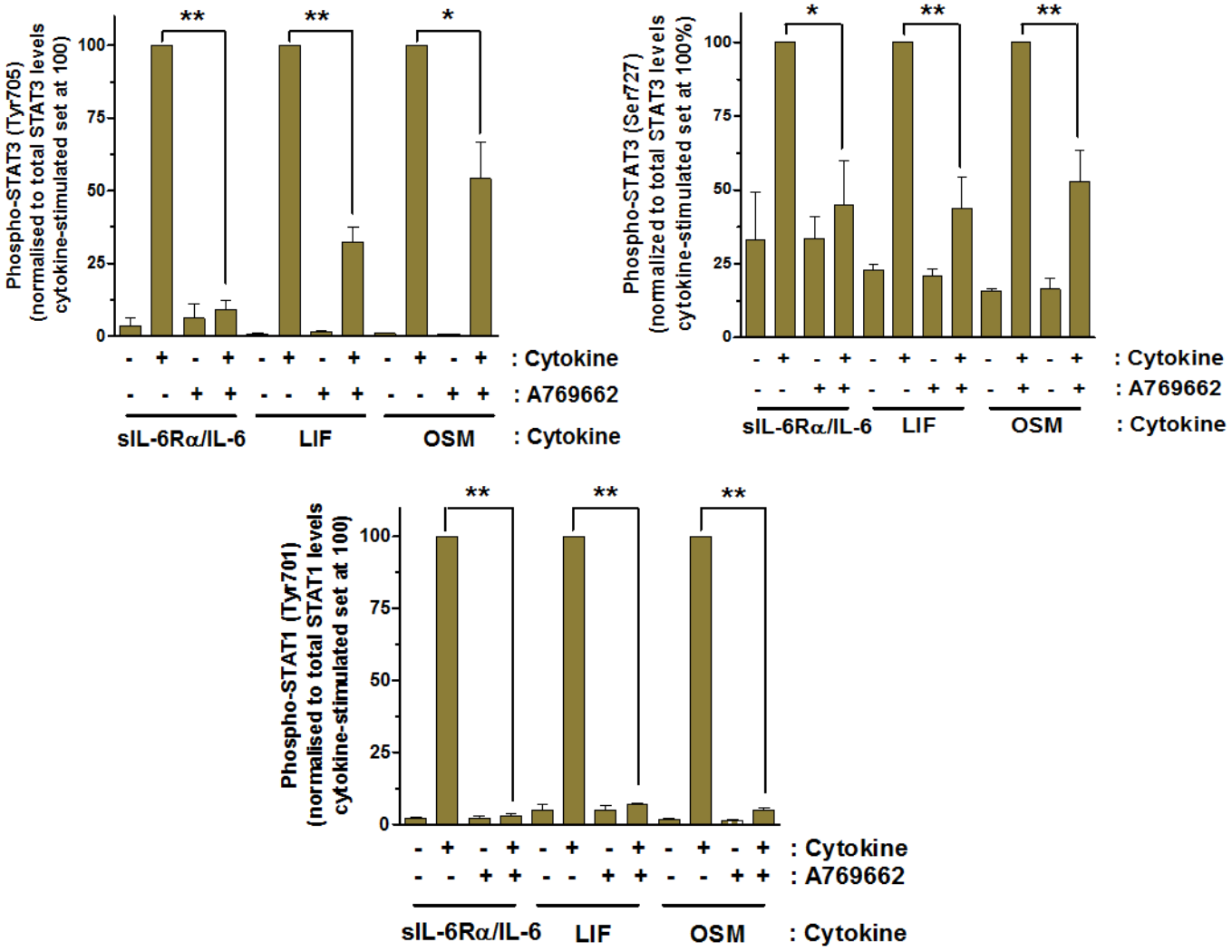
Phospho-STAT3 (Tyr705)
(normalised to total STAT3 levels
cytokine-stimulated set at 100)
Phospho-STAT3 (Ser727)
(normalized to total STAT3 levels
cytokine-stimulated set at 100%)
Phospho-STAT1 (Tyr701)
(normalised to total STAT1 levels
cytokine-stimulated set at 100)
0
25
50
75
100
**
*
: Cytokine
: A769662
sIL-6Rα/IL-6
LIF
OSM

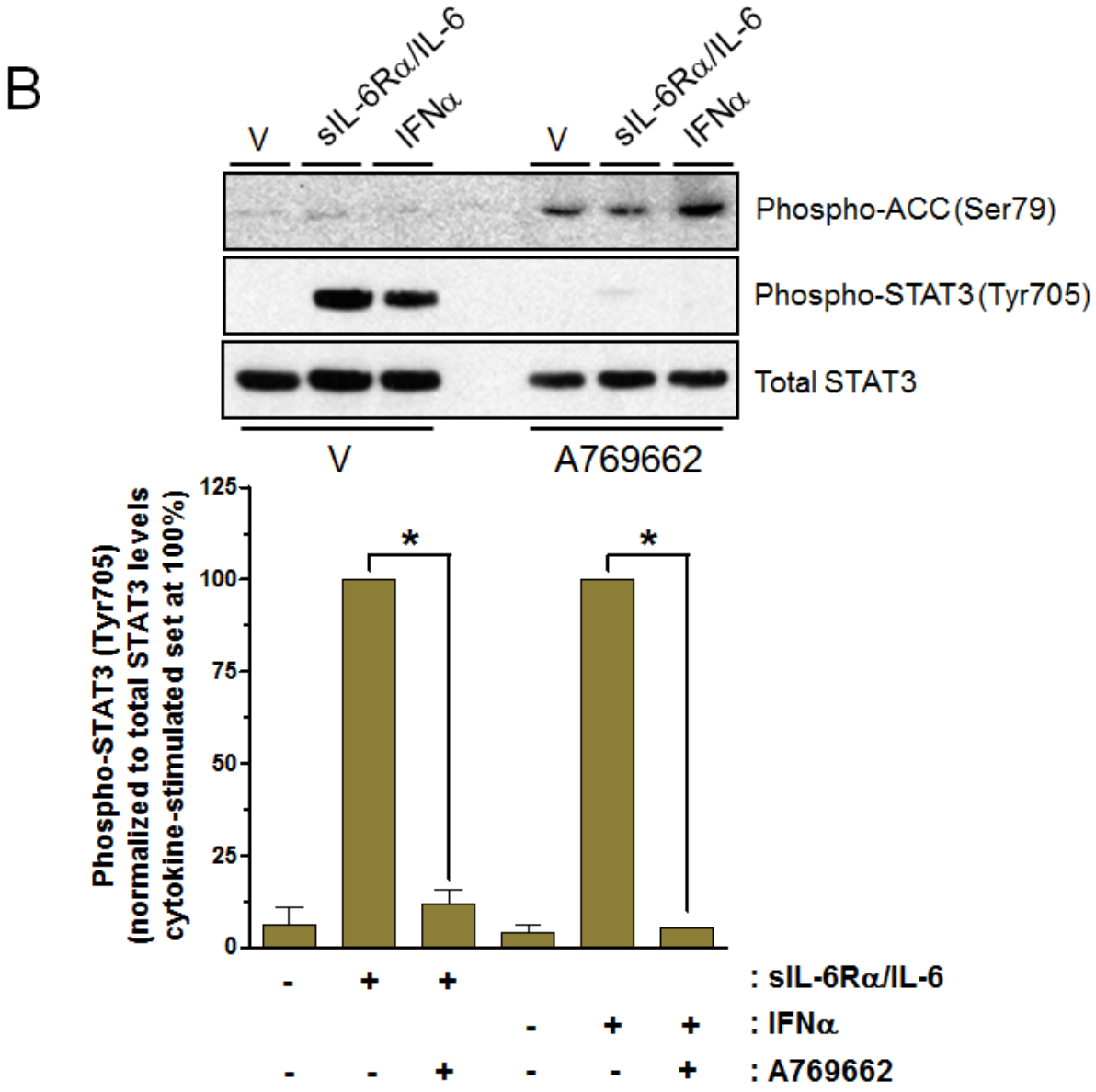

Fig. 2. AMPK inhibits STAT1 and STAT3 activation by IL-6, LIF, OSM and IFNα. (**A**) HUVECs were incubated for 30 min with either vehicle (V) or A769662 (100 μM) prior to stimulation with either vehicle (-), sIL-6Rα/IL-6 (25 ng/ml, 5 ng/ml), leukemia inhibitory factor (LIF: 10 ng/ml) or oncostatin M (OSM: 10 ng/ml) for 30 min. Cell lysates were then analyzed by SDS-PAGE and immunoblotting with the indicated antibodies. Densitometric analysis for STAT1 and STAT3 phosphorylation at the indicated sites normalized to respective total levels is shown in each case. Data are shown as mean ±SEM for N=4 independent experiments. **p<0.001. *p<0.01. (**B**) HUVECs were incubated for 30 min with either vehicle (V) or A769662 (100 μM) prior to

stimulation with either vehicle (V), sIL-6Rα/IL-6 (25 ng/ml, 5 ng/ml) for 30 min or IFNα (1000U/ml) for 15 min. Cell lysates were then analyzed by SDS-PAGE and immunoblotting with the indicated antibodies. Densitometric analysis for STAT3 phosphorylation normalized to respective total levels is shown in each case. Data are shown as mean ±SEM for N=3 independent experiments. *$p<0.001$.

A

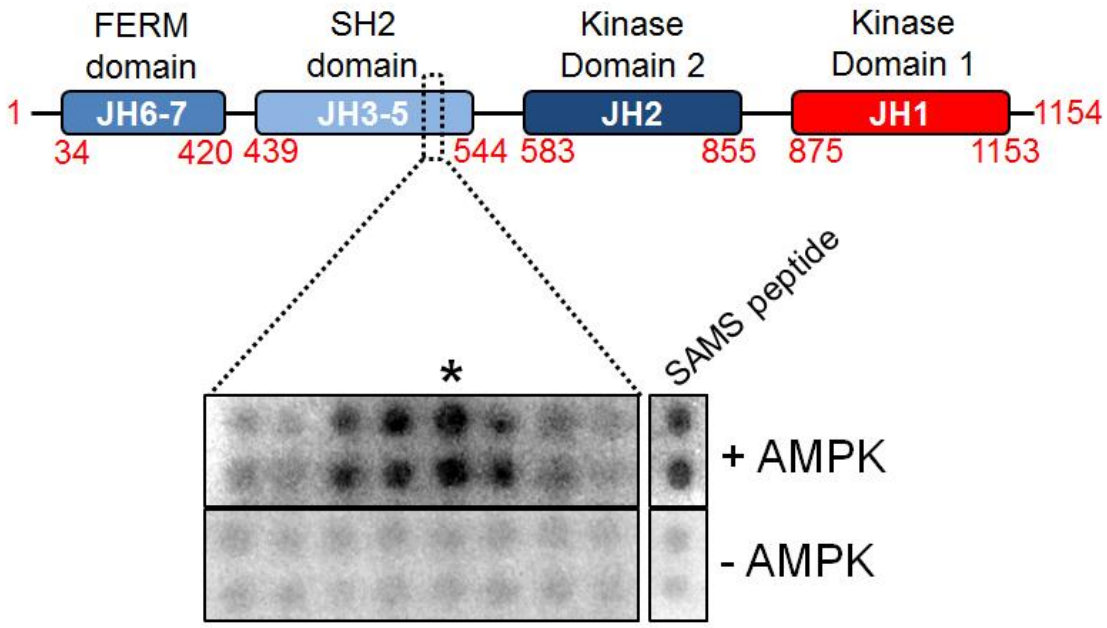

* = R[506]YSLHGSDRSFPSLGDLMSHLKKQI

B

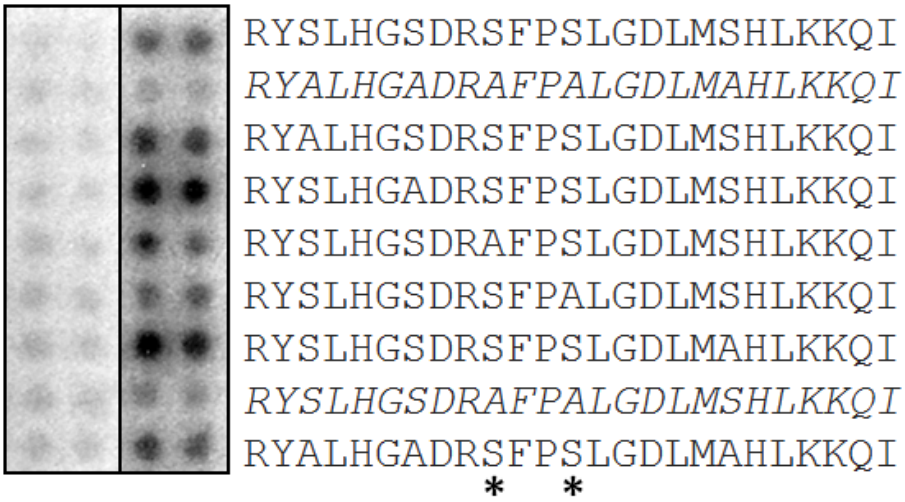

C

		-5 -4 -3 -2 -1 0 +1 +2 +3 +4
Optimal		LRRVXSXXNL
Secondary		MKKSXSXXDV
Additional		IXHRXSXXEI
Rat ACC1	Ser79	MRSSMSGLHL

Ser518 JAK1 site

Human JAK1	Ser518	DRSFPSLGDL
Mouse JAK1	Ser517	MDHFPSLRDL
Xenopus tropicalis JAK1	Ser504	DRGFDSLKDL
Danio rerio JAK1	Thr514	DTFRPTLKEL

Ser515 JAK1 site

Human JAK1	Ser515	HGSDRSFPSL

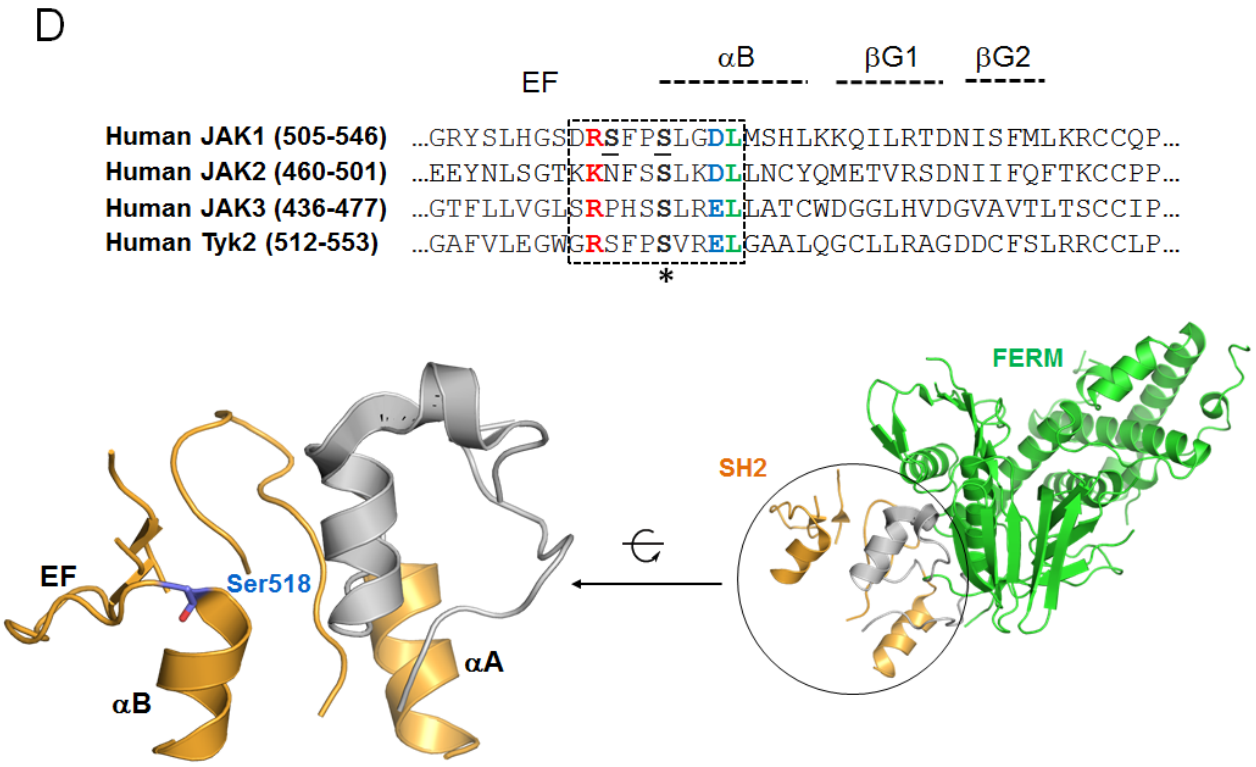

Fig. 3. Identification of Ser515 and Ser518 within the JAK1 SH2 domain as sites of AMPK phosphorylation *in vitro* (**A**) Overlapping peptide arrays spanning the human JAK1 open reading frame were subject to phosphorylation following incubation with [γ-^{32}P]ATP in the absence (-) or presence (+) of purified rat liver AMPK. The region of the array in which AMPK-dependent phosphorylation was detectable *versus* the no kinase control, and the location of the sequence within the domain structure of JAK1, is shown. Phosphorylation of immobilized SAMS peptide on the same array is also shown for comparison. This is representative of three experiments. (**B**) Immobilized peptides comprising WT and Ser/Ala-mutated versions of the indicated JAK1 sequence were subject to phosphorylation with [γ-^{32}P]ATP in either the absence (-) or presence (+) of purified AMPK as described in panel A. Peptides in italics are those which displayed no detectable phosphorylation above parallel arrays incubated without purified AMPK. The positions of Ser515 and Ser 518 are indicated by asterisks (*) This is representative of three experiments. **(C)** Optimal and secondary selections for AMPK substrate recognition taken from ref. 38. The sequence from rat ACC1 known to be phosphorylated by AMPK at Ser79 is shown for comparison. The conformity of the sequence surrounding Ser518 on human JAK1 to the AMPK consensus, and its evolutionary conservation, are shown. The sequence surrounding the Ser515 site on human JAK1 is also shown. The underlined Ser residue (equivalent to Ser518) indicates that this sequence would potentially conform

to a weak AMPK consensus site following the acquisition of negative charge upon its phosphorylation. (**D**) Upper: Alignment of SH2 domains from the four human JAK isoforms was performed using T-Coffee before being modified to match the structural data available for JAK1, JAK2 and Tyk2 *(39–41)*. For clarity, only the alignment of the indicated regions within each SH2 domain is shown. The lettering above the alignment indicates secondary structural elements, including the βG1 and βG2 regions present in the JAK2 and Tyk2 SH2 domains which are moderately disordered in the only available JAK1 SH2 domain structure *(39)*. The residues corresponding to Ser515 and 518 in JAK1 are underlined in bold, and the conserved Ser residues in JAK2, JAK3 and Tyk2 equivalent to Ser518 are in bold and highlighted underneath with an asterisk (*). Residues in the boxed region highlighting sequences surrounding the conserved Ser residue in each JAK isoform are color coded similar to Panel C to show conformity to the AMPK consensus. Lower: The right hand figure shows the structure of the human JAK1 FERM-SH2 fusion (PDB: 5IXD) generated using PyMol *(39)*. The enlarged SH2 domain structure on the left hand side shows the location of Ser518 within the αB helix immediately downstream of the EF loop. The αA loop present in all SH2 domains is also indicated.

A

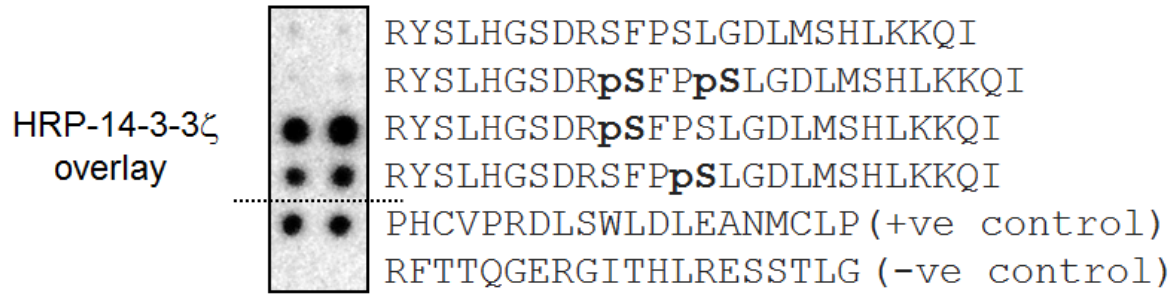
HRP-14-3-3ζ
overlay
RYSLHGSDRSFPSLGDLMSHLKKQI
RYSLHGSDRpSFPpSLGDLMSHLKKQI
RYSLHGSDRpSFPSLGDLMSHLKKQI
RYSLHGSDRSFPpSLGDLMSHLKKQI
PHCVPRDLSWLDLEANMCLP (+ve control)
RFTTQGERGITHLRESSTLG (-ve control)

B

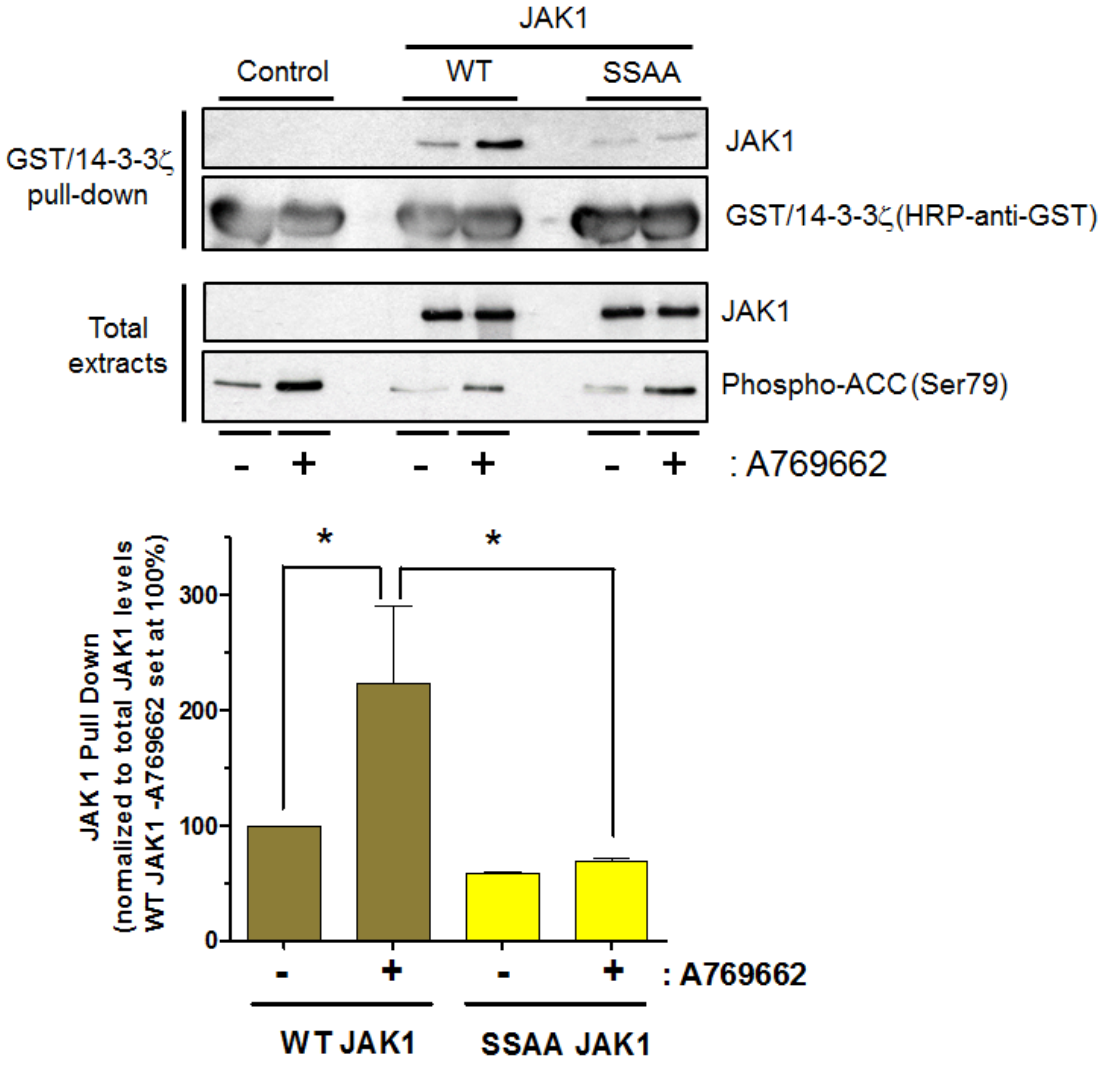
JAK1
Control
WT
SSAA
GST/14-3-3ζ pull-down
JAK1
GST/14-3-3ζ(HRP-anti-GST)
Total extracts
JAK1
Phospho-ACC(Ser79)
- + - + - + : A769662
JAK 1 Pull Down (nomalized to total JAK1 levels WT JAK1 -A769662 set at 100%)
300
200
100
0
*
*
- + - + : A769662
WT JAK1
SSAA JAK1

C

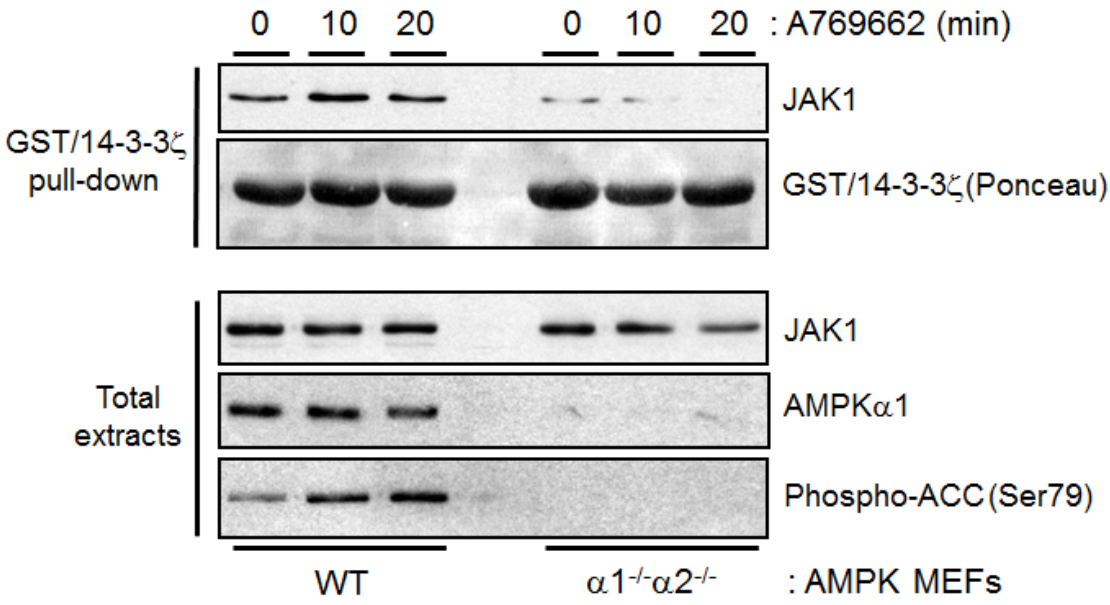
0 10 20 0 10 20 : A769662 (min)
GST/14-3-3ζ pull-down
JAK1
GST/14-3-3ζ(Ponceau)
Total extracts
JAK1
AMPKα1
Phospho-ACC(Ser79)
WT
α1-/-α2-/-
: AMPK MEFs

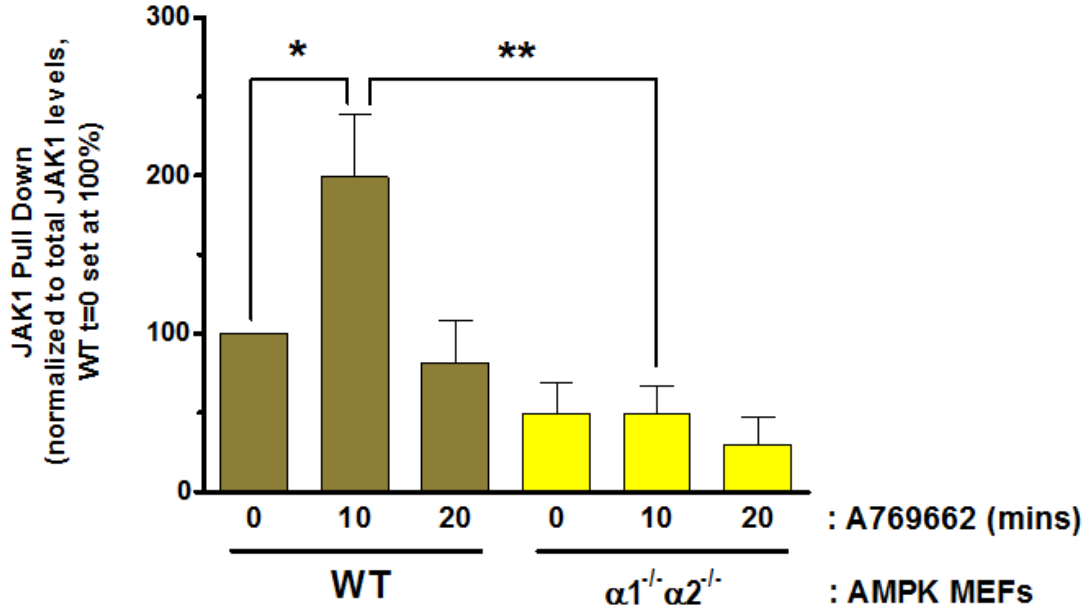
JAK1 Pull Down
(normalized to total JAK1 levels,
WT t=0 set at 100%)
300
200
100
0
*
**
0 10 20 0 10 20
: A769662 (mins)
WT
α1-/-α2-/-
: AMPK MEFs

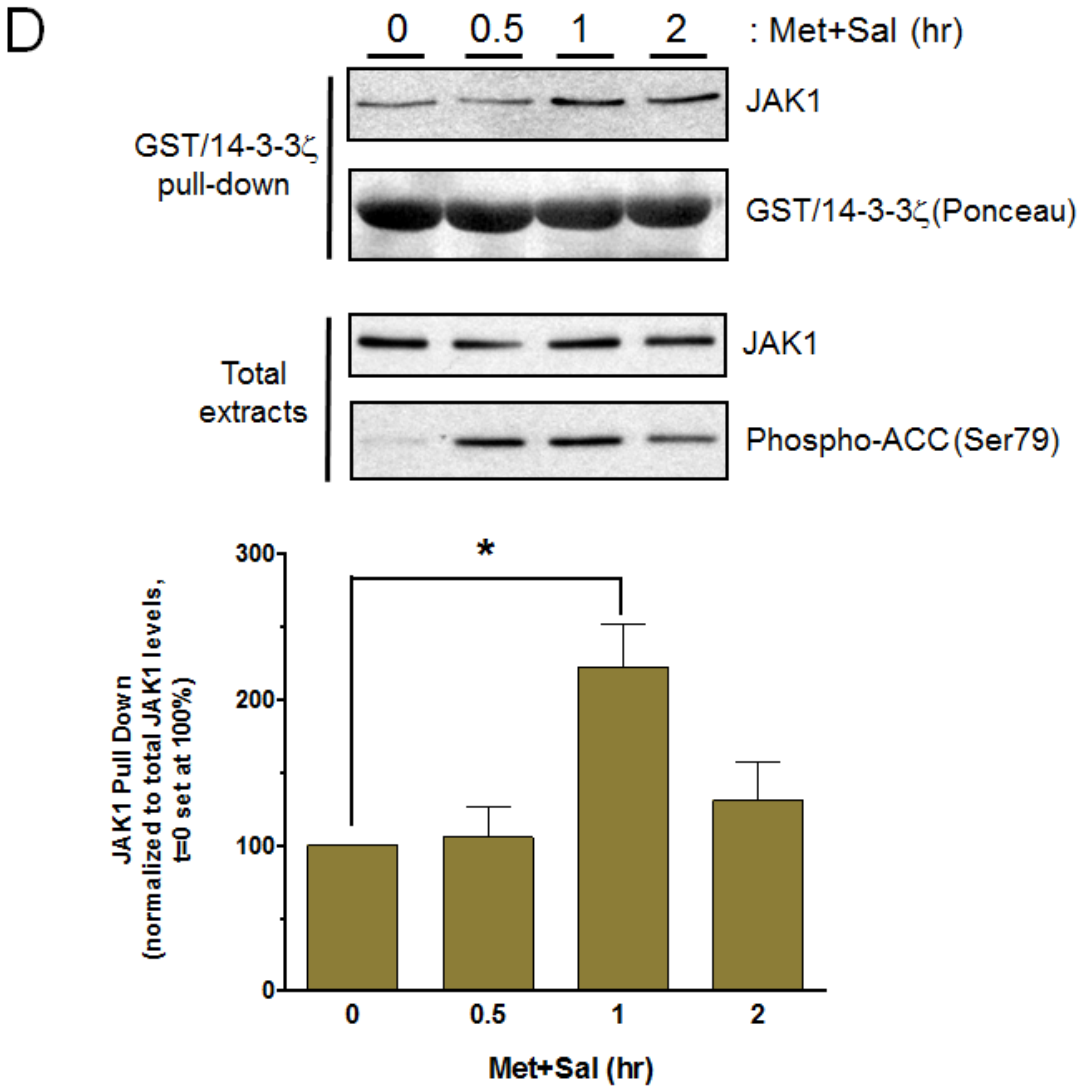

Fig. 4 AMPK-mediated phosphorylation of JAK1 in intact cells. (**A**) Immobilized peptides comprising the indicated JAK1 sequence and variants with phosphorylated and non-phosphorylated versions of Ser515 and Ser518 were overlaid with HRP-conjugated 14-3-3ζ as indicated. Positive and negative control peptides for 14-3-3ζ interaction *(74)* are also shown. This is representative of N=3 experiments. (**B**) JAK1-null U4C human fibrosarcoma cells were transiently transfected with WT JAK1 or Ser515,518Ala (SSAA) JAK1 constructs versus a control transfection (Control) and treated with or without A769662 (100 μM) for 40 min as indicated. 10% of each total cell extract was used for immunoblotting with the indicated antibodies. The remainder was incubated with GST/14-3-3ζ and glutathione-Sepharose beads. Captured JAK1 was detected by immunoblotting with anti-JAK1 antibody as indicated. Densitometric analysis for JAK1

pull down normalized to respective total levels is shown in each case. Data are shown as mean ±SEM for N=3 independent experiments. **p<0.01, *p<0.05. (**C**) Immortalized WT and AMPKα1$^{-/-}$α2$^{-/-}$ MEFs were treated with A769662 (100 μM) for the indicated times. 10% of each total extract was used for immunoblotting with the indicated antibodies. The remainder was incubated with GST/14-3-3ζ and glutathione-Sepharose beads. Captured endogenous JAK1 was detected by immunoblotting with anti-JAK1 antibody as indicated. Densitometric analysis for JAK1 pull down normalized to respective total levels is shown in each case. Data are shown as mean ±SEM for N=3 independent experiments. *p<0.05. (**D**) HUVECs were treated for the indicated times with metformin (3 mM) and salicylate (5 mM) (Met+Sal). 10% of each total extract was used for immunoblotting with the indicated antibodies. The remainder was incubated with GST/14-3-3ζ and glutathione-Sepharose beads. Captured JAK1 was detected by immunoblotting with anti-JAK1 antibody as indicated. Densitometric analysis of N=3 independent experiments for JAK1 pull down normalized to respective total levels in each condition is shown. *p<0.05.

A

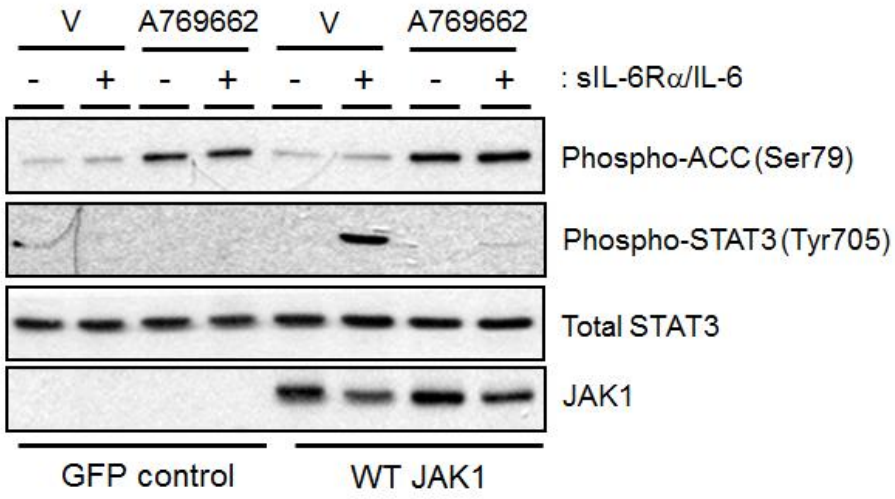
V
A769662
V
A769662
- + - + - + - +
: sIL-6Rα/IL-6
Phospho-ACC (Ser79)
Phospho-STAT3 (Tyr705)
Total STAT3
JAK1
GFP control
WT JAK1

B

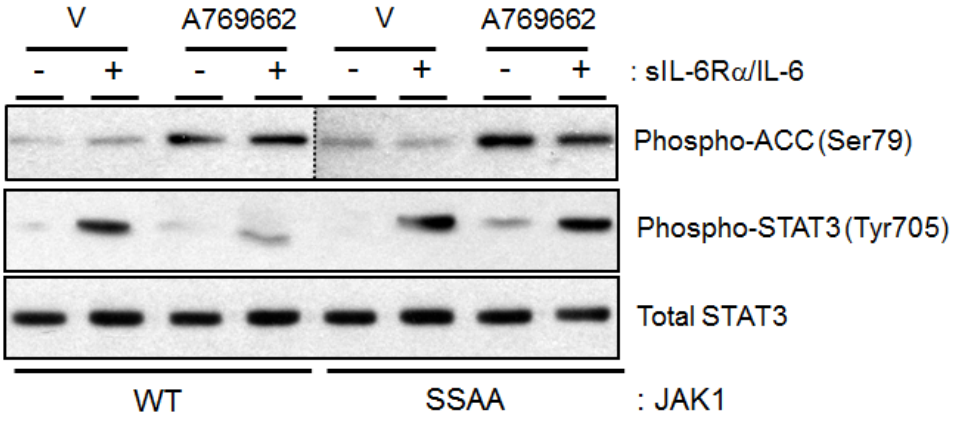
V
A769662
V
A769662
- + - + - + - +
: sIL-6Rα/IL-6
Phospho-ACC (Ser79)
Phospho-STAT3 (Tyr705)
Total STAT3
WT
SSAA
: JAK1

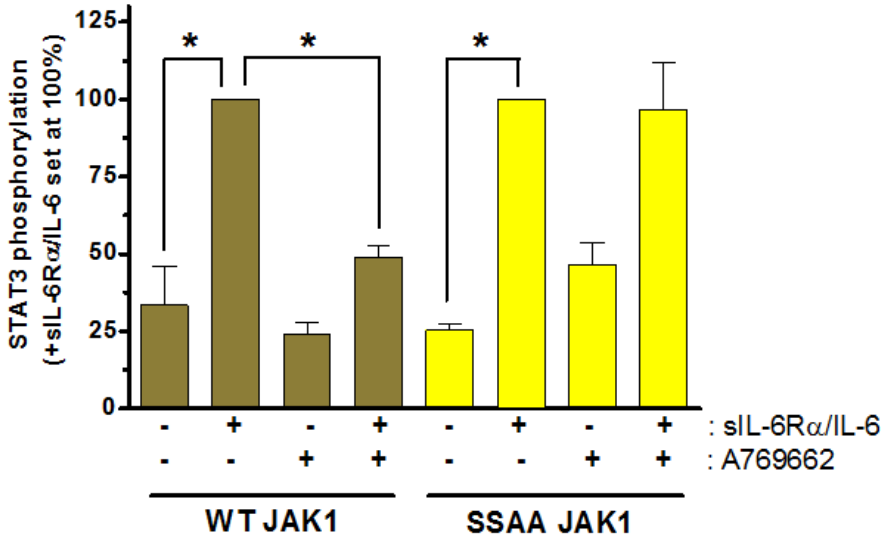
STAT3 phosphorylation
(+sIL-6Rα/IL-6 set at 100%)
125
100
75
50
25
0
*
*
*
- + - + - + - +
: sIL-6Rα/IL-6
- - + + - - + +
: A769662
WT JAK1
SSAA JAK1

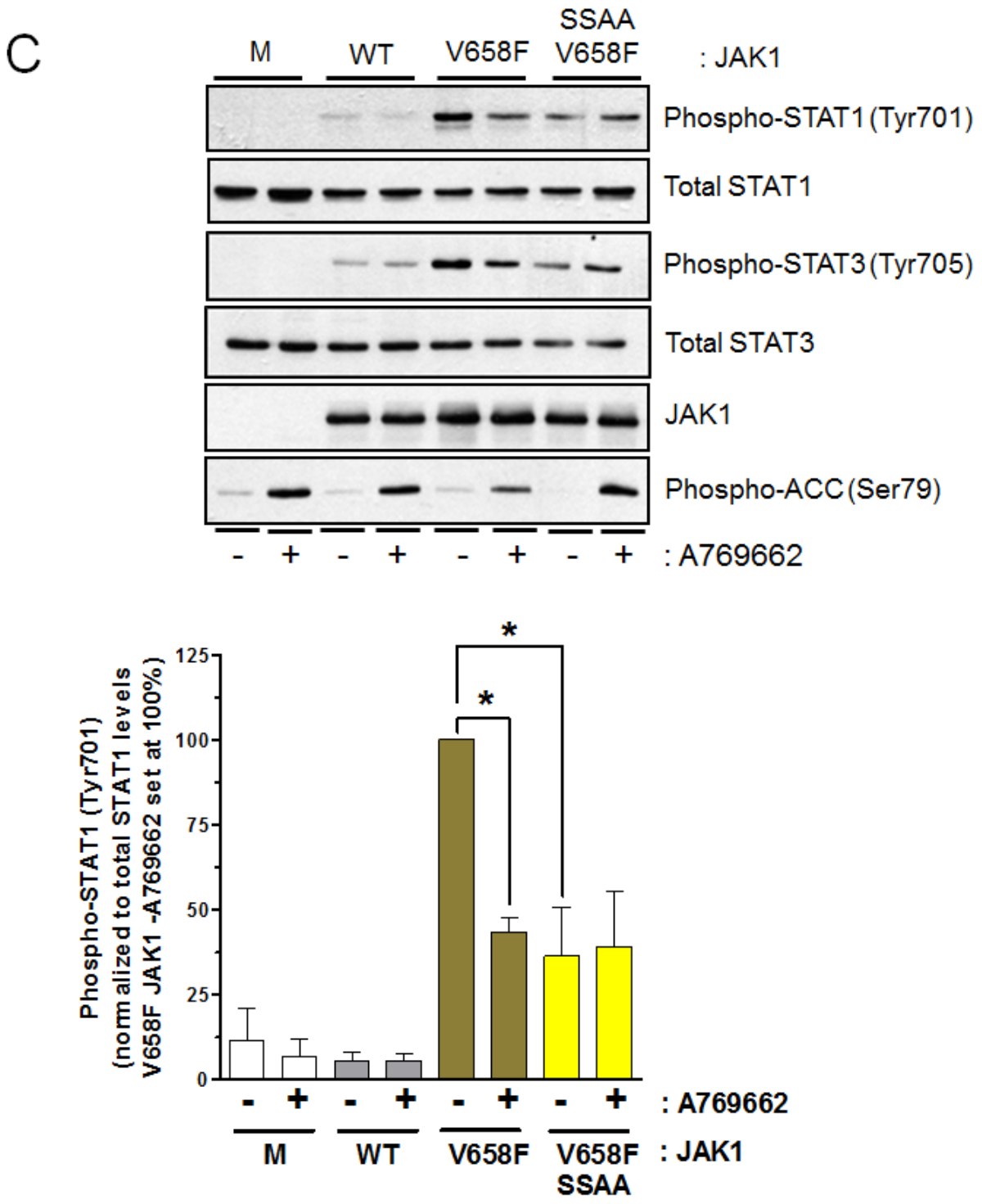

Fig. 5 AMPK-mediated inhibition of JAK1-dependent signaling requires Ser515 and Ser518. (**A**) JAK1-null U4C cells were transiently transfected with either control GFP or WT JAK1 constructs and treated with or without sIL-6Rα/IL-6 (25 ng/ml, 5 ng/ml) for 30 min following a pre-incubation with or without A769662 (100 μM) for 40 min as

indicated. Protein-equalized cell lysates were then analyzed by SDS-PAGE and immunoblotting with the indicated antibodies. This is representative of N=4 experiments. (**B**) U4C cells were transiently transfected with either WT JAK1 or Ser515,518Ala (SSAA) JAK1 constructs and treated with or without sIL-6Rα/IL-6 (25 ng/ml, 5 ng/ml) for 30 min following a pre-incubation with or without A769662 (100 μM) for 30 min as indicated. Protein-equalized cell lysates were then analyzed by SDS-PAGE and immunoblotting with the indicated antibodies. The dotted line indicates where unrelated lanes were removed for clarity. Densitometric analysis of STAT3 phosphorylation normalized to respective total levels is shown in each case. Data are shown as mean ±SEM for N=3 independent experiments. *$p<0.001$. (**C**) U4C cells were transiently transfected with either WT JAK1, Val658Phe JAK1 (V658F) or Ser515,518Ala Val658Phe JAK1 (V658F SSAA) constructs prior to treatment with or without A769662 (100 μM) for 30 min as indicated. Protein-equalized cell lysates were then analyzed by SDS-PAGE and immunoblotting with the indicated antibodies. Densitometric analysis of STAT1 phosphorylation normalized to respective total levels is shown in each case. Data are shown as mean ±SEM for N=3 independent experiments. *$p<0.01$.

Supplementary Materials for

Rapid AMP-activated protein kinase (AMPK) phosphorylation of Janus kinase 1 (JAK1) links energy sensing to anti-inflammatory signaling

Claire Rutherford, Claire Speirs, Jamie J.L. Williams, Marie-Ann Ewart, Sarah J. Mancini, Simon A. Hawley, Christian Delles, Benoit Viollet, Ana P. Costa-Pereira, George S. Baillie, Ian P. Salt* and Timothy M. Palmer*

*Corresponding authors: E mail: T.Palmer1@bradford.ac.uk, Ian.Salt@glasgow.ac.uk

This file includes:-

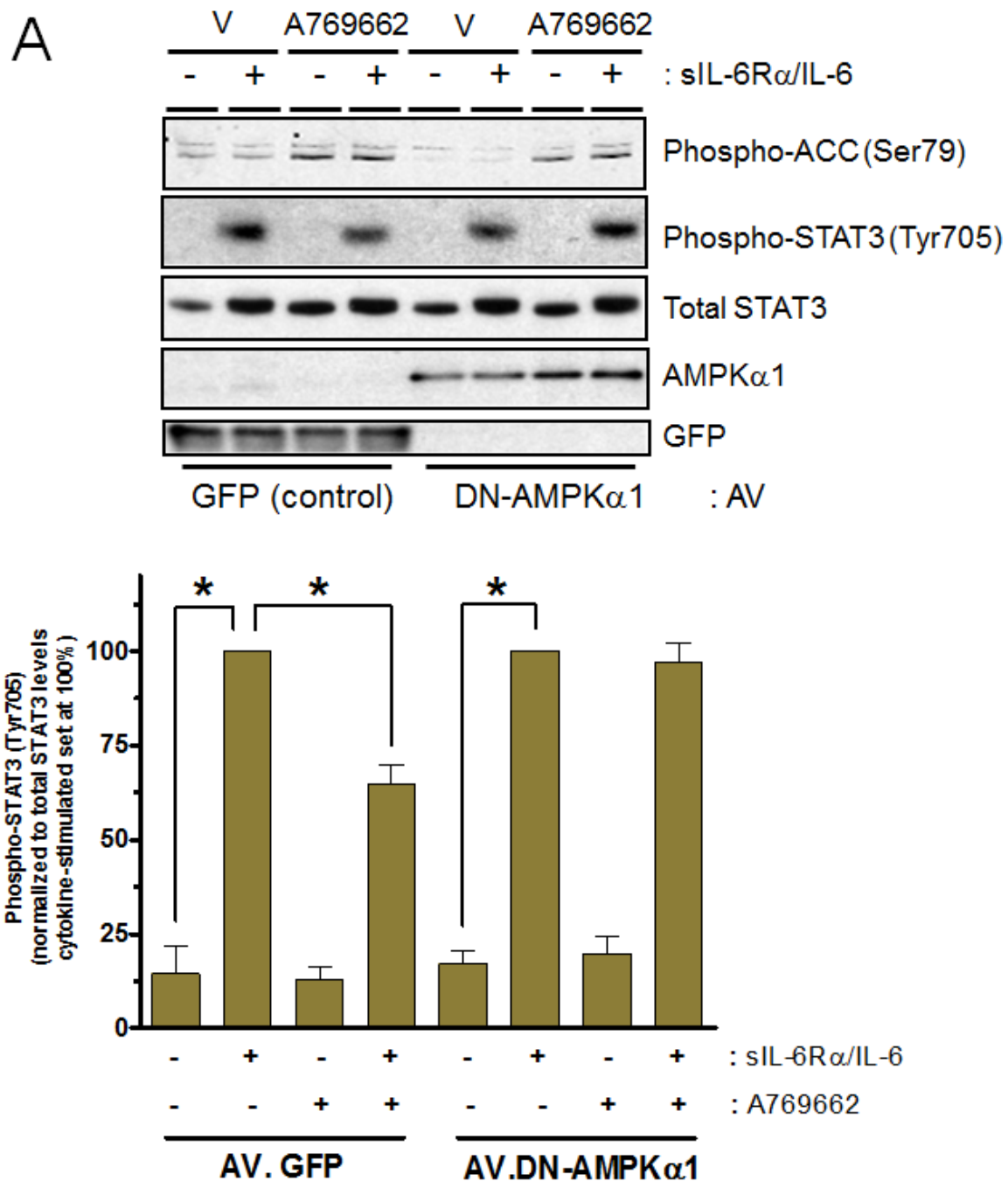
A
V
A769662
V
A769662
- + - + - + - +
: sIL-6Rα/IL-6
Phospho-ACC (Ser79)
Phospho-STAT3 (Tyr705)
Total STAT3
AMPKα1
GFP
GFP (control)
DN-AMPKα1
: AV
Phospho-STAT3 (Tyr705)
(normalized to total STAT3 levels
cytokine-stimulated set at 100%)
100
75
50
25
0
*
*
*
- + - + - + - +
: sIL-6Rα/IL-6
- - + + - - + +
: A769662
AV. GFP
AV.DN-AMPKα1

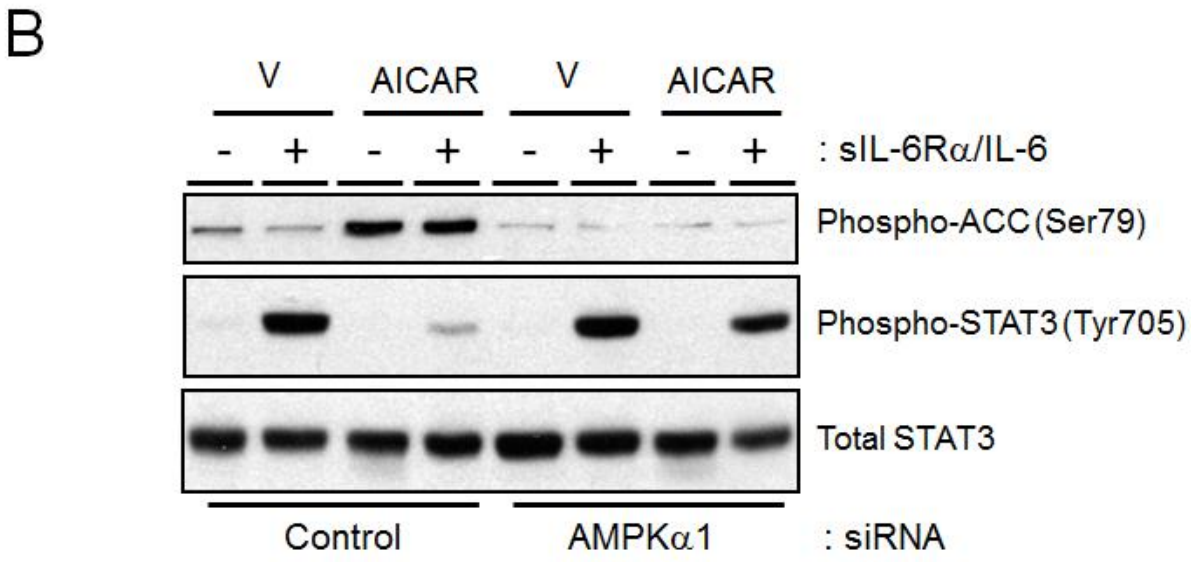

Fig. S1 AMPK-dependence of inhibition of STAT3 phosphorylation in HUVECs. (**A**) HUVECs were infected with control (GFP) or DN-AMPKα1-expressing adenovirus (AV) prior to treatment with or without sIL-6Rα/IL-6 (25 ng/ml, 5 ng/ml) for 30 min following a pre-incubation with or without A769662 (100 μM) for 40 min as indicated.. Protein-equalized cell lysates were then analyzed by SDS-PAGE and immunoblotting with the indicated antibodies. The immunoblots shown are representative of multiple experiments. (**B**) HUVECs were pre-incubated in the presence or absence of 1 mM AICAR (2 hr) prior to stimulation with sIL-6Rα/IL-6 (25 ng/ml, 5 ng/ml) for a further 30 min as indicated. Protein-equalized cell lysates were then analyzed by SDS-PAGE and immunoblotting with the indicated antibodies. The data shown are representative of multiple experiments.

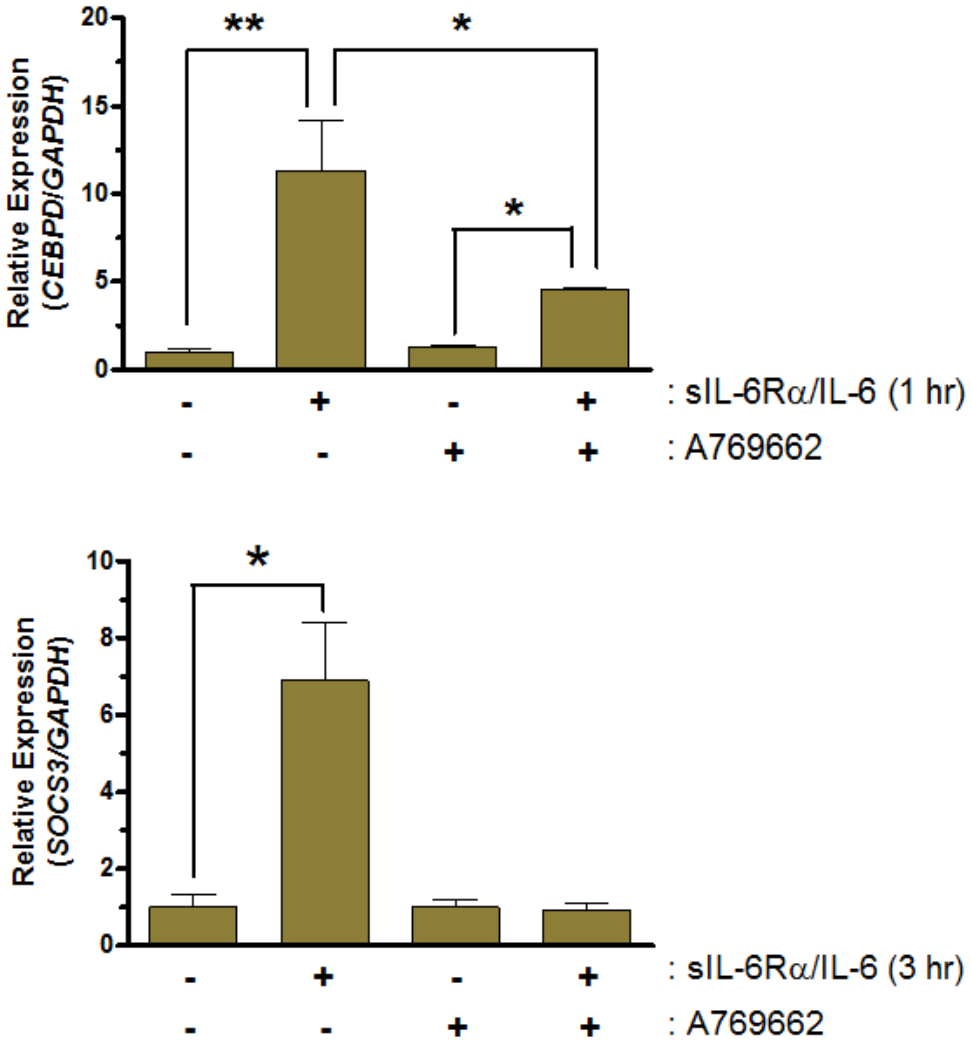

Fig. S2. AMPK inhibition of sIL-6Rα/IL-6-mediated *SOCS3* and *CEBPD* mRNA induction. HUVECs were pre-treated for 30 min with or without A769662 (100 μM) prior to stimulation with sIL-6Rα/IL-6 (25 ng/ml, 5 ng/ml) for either 1 hr (*CEBPD*) or 3 hr (*SOCS3*). Messenger RNA levels were then analyzed by quantitative reverse transcription PCR and normalized to *GAPDH* mRNA. Analysis of N=3 (*CEBPD*) or N=4 (*SOCS3*) independent experiments for *SOCS3* and *CEBPD* normalized to *GAPDH* levels is shown. For the *CEBPD* graph, *p<0.01, **p<0.001. For the *SOCS3* graph, *p<0.001.

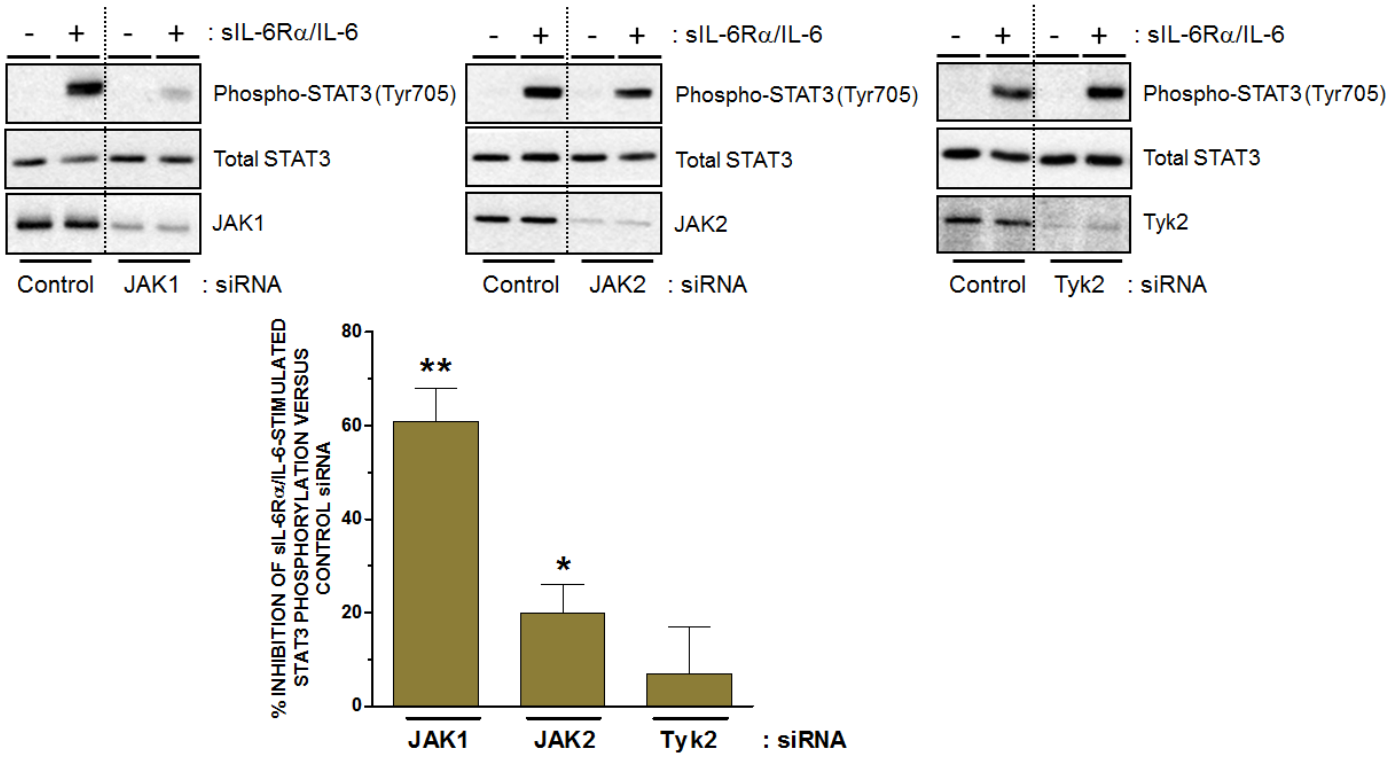

Fig. S3. Contributions of JAK1, JAK2 and Tyk2 towards mediating sIL-6Rα/IL-6-mediated STAT3 phosphorylation in HUVECs. (**A**) HUVECs were transfected with either control or JAK isoform-targeted siRNAs as indicated prior to stimulation with or without sIL-6Rα/IL-6 (25 ng/ml, 5 ng/ml) for 30 min. Protein-equalized cell lysates were then analyzed by SDS-PAGE and immunoblotting with the indicated antibodies. The dotted lines indicate where unrelated lanes were removed for clarity. Densitometric analysis for inhibition of sIL-6Rα/IL-6-stimulated STAT3 phosphorylation normalized to respective total levels are shown for each of JAK1, JAK2 and Tyk2. Data are shown as mean ±SEM for N=3 (Tyk2), N=4 (JAK2) or N=5 (JAK1) independent experiments. **p<0.001, *p<0.01.

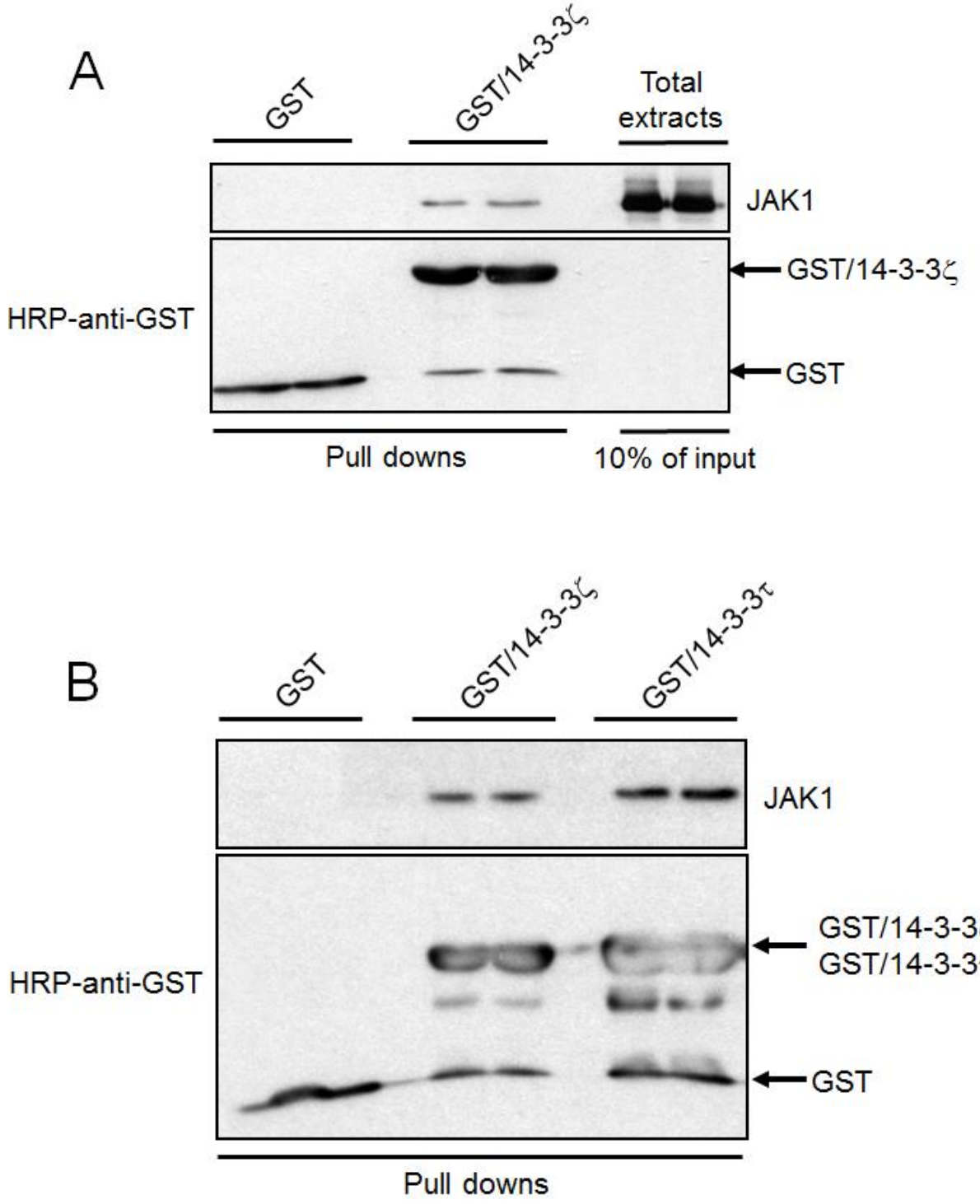
A
GST
GST/14-3-3ζ
Total extracts
JAK1
HRP-anti-GST
GST/14-3-3ζ
GST
Pull downs
10% of input
B
GST
GST/14-3-3ζ
GST/14-3-3τ
JAK1
HRP-anti-GST
GST/14-3-3ζ
GST/14-3-3τ
GST
Pull downs

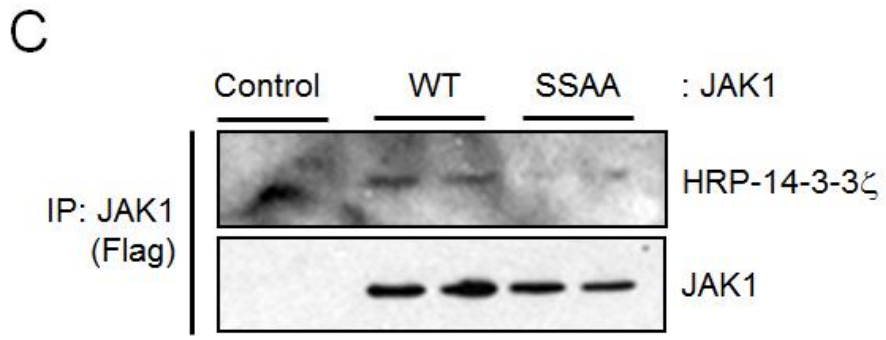

Fig. S4. Specific interaction of JAK1 with 14-3-3ζ and τ. (**A**) JAK1-null U4C cells in which JAK1 was stably re-expressed were lysed and protein-equalized soluble extracts incubated with either GST or GST/14-3-3ζ and glutathione-Sepharose beads. Captured JAK1 and total JAK1 present in 10% of the total extracts used for the pull down assay were detected by immunoblotting with anti-JAK1 antibody, while recovered GST and GST/14-3-3ζ were identified by HRP-conjugated anti-GST as indicated. The data shown are representative of multiple experiments. (**B**) JAK1-null U4C cells in which JAK1 was stably re-expressed were lysed and protein-equalized soluble extracts incubated with either GST, GST/14-3-3ζ or GST/14-3-3τ and glutathione-Sepharose beads. Captured JAK1 was detected by immunoblotting with anti-JAK1 antibody, while recovered GST fusion proteins were identified by HRP-conjugated anti-GST as indicated. The data shown are representative of multiple experiments. (C) U4C cells transiently transfected with either WT JAK1 or Ser515,518Ala (SSAA) JAK1 constructs were lysed and protein-equalized soluble extracts incubated with anti-Flag antibody to immunoprecipitate recombinant JAK1. Immunoprecipitates were probed with HRP-conjugated 14-3-3ζ then re-probed with anti-JAK1 antibody as indicated. The data shown are representative of multiple experiments.